6.c. A more complex simulated dataset

The second simulated dataset, A2, addresses a scenario more closely approximating Tanner crab data in the assessment. It incorporates four simulated fisheries (loosely based on the directed Tanner crab, snow crab bycatch, Bristol Bay red king crab bycatch, and groundfish trawl bycatch fisheries) and a single abundance survey (loosely based on the annual NMFS EBS bottom trawl survey), as in the assessment. The rsimTCSAM model configuration file, "rsimTCSAM.Configuration.A2.dat", is available on GitHub at the following URL: https://github.com/wStockhausen/rsimTCSAM.git. Comprehensive plots of model results are provided in the accompanying online material in the file 'rsimTCSAM.A2.pdf'.

The principal population dynamics underlying A2 were the same as those for A1 (see Section 6a). The only difference was that natural mortality rates were sex- and maturity state-specific and they varied between two time blocks (Fig. 6c.1). Otherwise the differences between the two simulations were in how fisheries and surveys were handled.

Four simulated fisheries were defined for A2, loosely based on the Tanner crab assessment in terms of selectivity functions, retention functions, discard mortality rates, and periods over which the fisheries were open or closed. For A2, the simulated fisheries were: 1) 'TCF', the Tanner crab fishery; 2) 'SCF', the snow crab fishery; 3) 'RKF', the Bristol Bay red king crab fishery; and 4) 'GTF', the groundfish trawl fishery. Only TCF was a directed fishery with retention of legal-sized males—the other fisheries were bycatch fisheries which discarded all Tanner crab taken incidental to their own targets (the targets are not modeled in the simulation). In addition to retaining legal-sized males, smaller males and all females captured in the TCF were discarded. Discard mortality was applied to discarded crab at rates of 32.1% for the crab captured in the simulated crab fisheries and 80% for those captured in the simulated trawl fishery.

The TCF directed fishery was started in 1965 and continued, with closures, until the end of the model period. Two time blocks with differing selectivity curves for males were defined for the TCF: a) 1965 to 1984 and b) 1987 to 2013 (Fig. 6c.2). The retention for males was the same across the two time blocks, as was the selectivity for females and median capture rates (0.3 yr^{-1}). All selectivity/retention curves were ascending logistic functions. Ln-scale deviations in capture rate were randomly generated for each time block, using a standard deviation of 0.4. The fishery was closed during 1985 and 1986, as well as from 1996 through 2004 and 2010 through 2012. The resulting fully-selected capture rates are shown in Fig. 6c.3.

The SCF bycatch fishery was started in 1978 and continued until the end of the model period. Three time blocks with differing bycatch selectivity curves for males and females were defined for SCF: a) 1978:1996, b) 1997-2004, and c) 2005-2013 (Fig. 6c.4). Male selectivity functions were double logistic functions, whereas females were ascending logistic functions. A median capture rate of 0.15 was used for both sexes in the first time block, while a rate of 0.1 was used in the latter two time blocks. Ln-scale deviations in capture rate were randomly generated for each time block, using a standard deviation of 0.4. The resulting fully-selected capture rates are shown in Fig. 6c.3.

The RKF bycatch fishery was started in 1978 and continued, with closures, until the end of the model period. Three time blocks with differing bycatch selectivity curves for males and females were defined for RKF: a) 1978-1996, b) 1997-2004, and c) 2005-2013 (Fig. 6c.5). All selectivity curves were ascending

logistic functions. Median capture rates of 0.10, 0.05, and 0.01 were applied to both sexes in the three time blocks, respectively. Ln-scale deviations in capture rate were randomly generated for each time block, using a standard deviation of 0.4. The fishery was closed in 1984 and 1985, and again in 1994 and 1995. The resulting fully-selected capture rates are shown in Fig. 6c.3.

The GTF trawl bycatch fishery was started in 1973 and continued until the end of the model period. Three time blocks with differing bycatch selectivity curves for males and females were defined for RKF: a) 1973-1986, b) 1987-1996, and c) 1997-2013 (Fig. 6c.5). All selectivity curves were ascending logistic functions. Median capture rates of 0.15, 0.10, and 0.05 were applied to both sexes in the three time blocks, respectively. Ln-scale deviations in capture rate were randomly generated for each time block, using a standard deviation of 0.4. The resulting fully-selected capture rates are shown in Fig. 6c.3.

The simulated NMFS trawl survey was started in 1975 and "conducted" annually at the start of the crab year (July 1). Two time periods with differing selectivity curves were defined for the survey: a) 1975-1981 and b) 1982-2014 (Fig. 6c.7). Fully-selected catchability was sex-specific (1.0 for males, 0.8 for females) across both time blocks.

The initial size compositions for the simulation, based on the equilibrium considerations outlined in Section 4, are illustrated in Fig. 6c.8. The recruitment time series used to drive the simulation is shown in Fig. 6c.9. Strictly by chance, recruitment levels appear to increase over the extent of the model period. The resulting simulated population abundance and mature biomass time series are shown in Fig. 6c.10. Male abundance is higher than female abundance before the directed fishery starts in 1965 due to higher natural mortality rates on females.

The numbers of crab captured in the various fisheries, as well as the mortality associated with retention and discarding, is shown in Fig. 6c.11. Fig. 6c.12 shows the trends of simulated survey abundance and biomass.
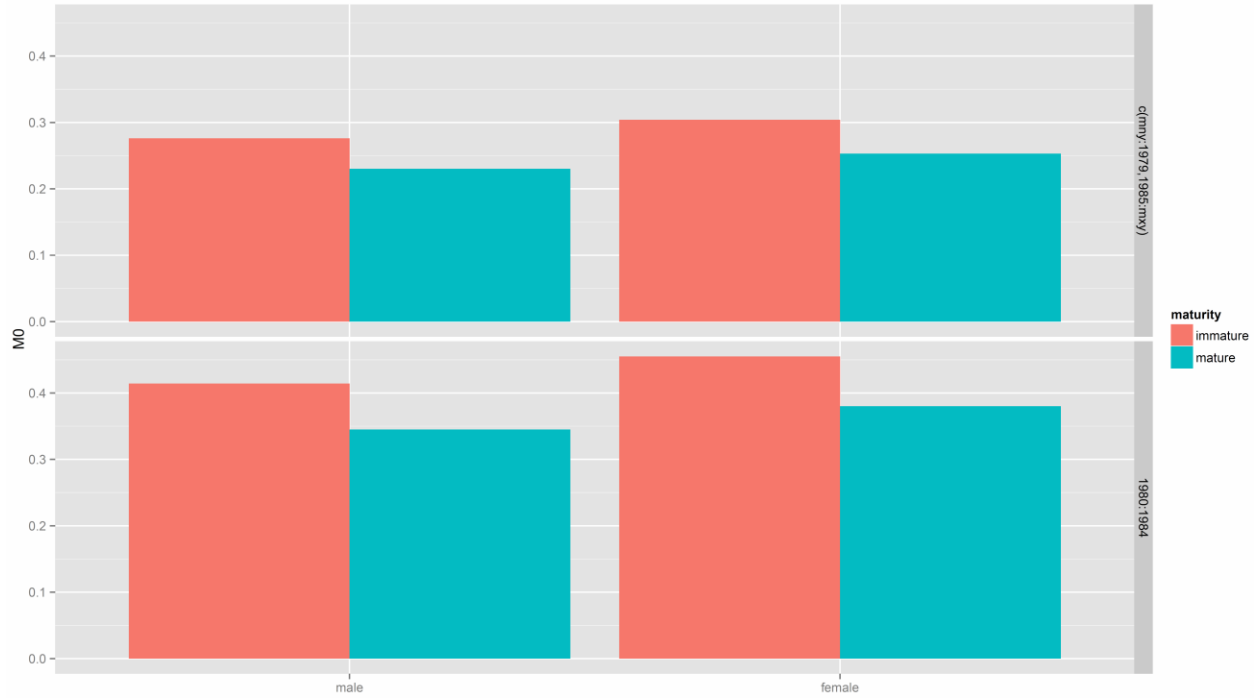
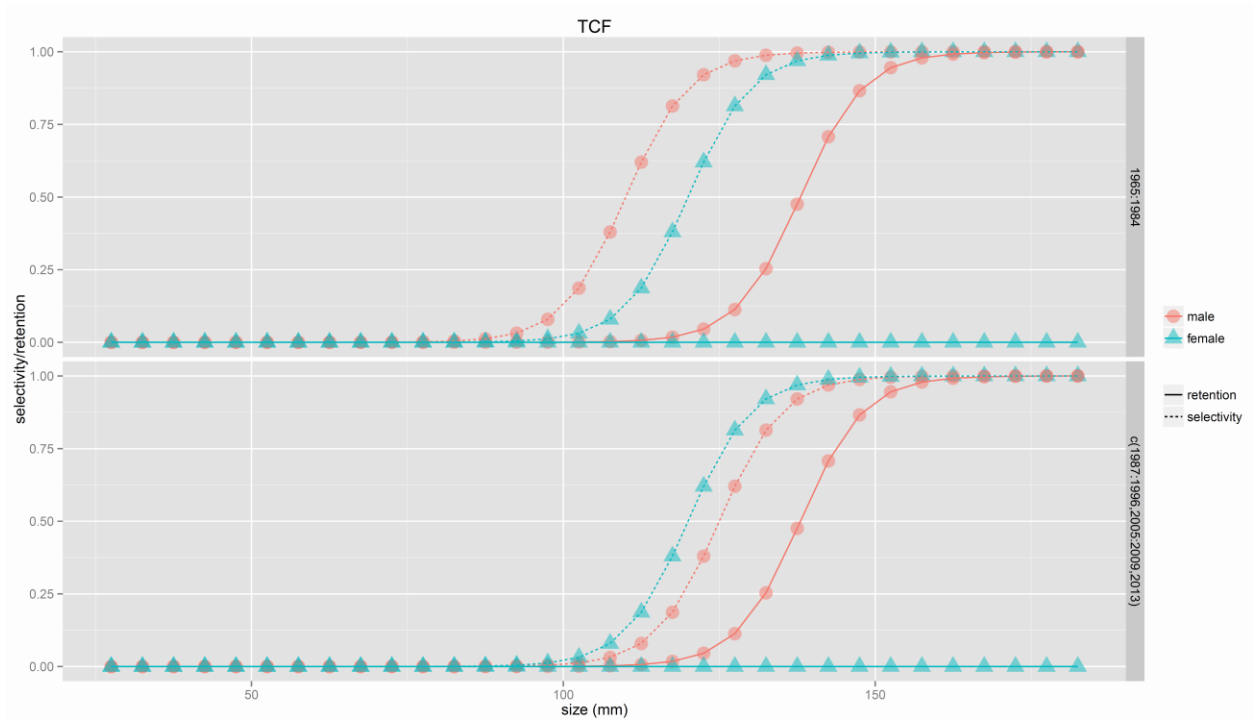Fig. 6c.1. Simulated natural mortality rates for two time blocks.

Fig. 6c.2. Selectivity and retention curves in two time blocks for the simulated directed crab fishery, TCF. Upper graph: 1965-1984. Lower graph: 1987-2013.
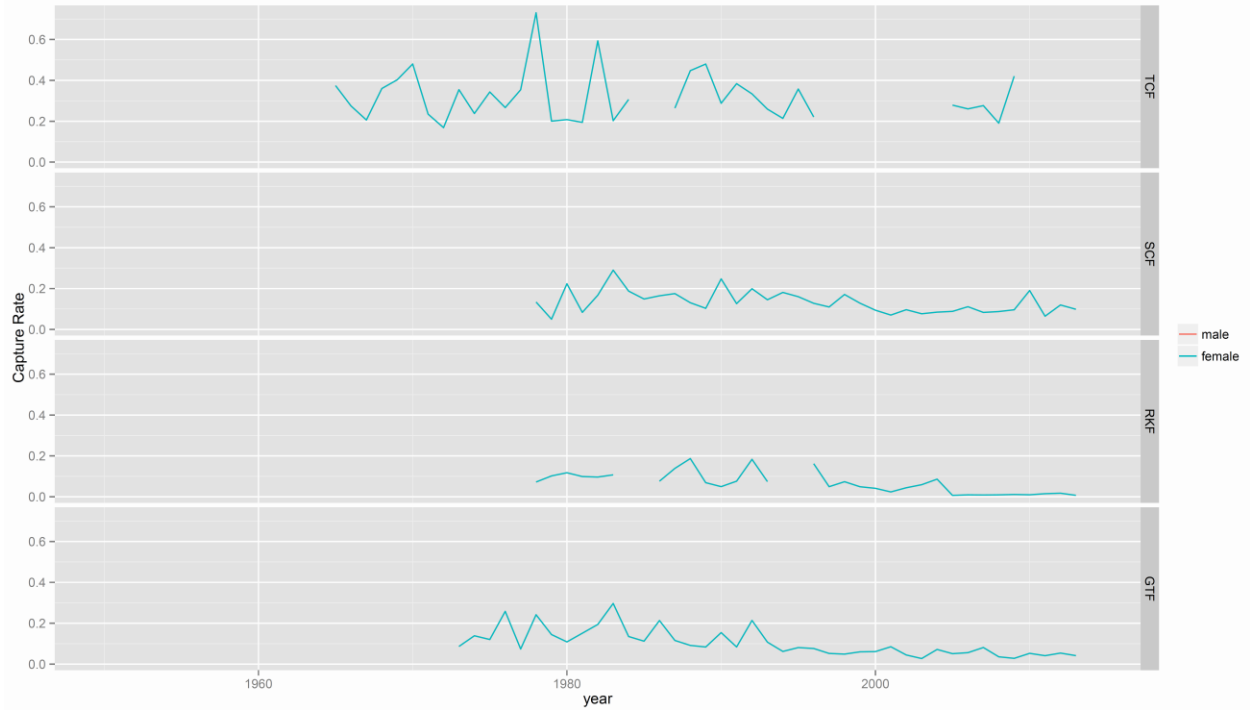
Fig. 6c.3. Fully-selected capture rates in the simulated fisheries. Male and female capture rates are identical.
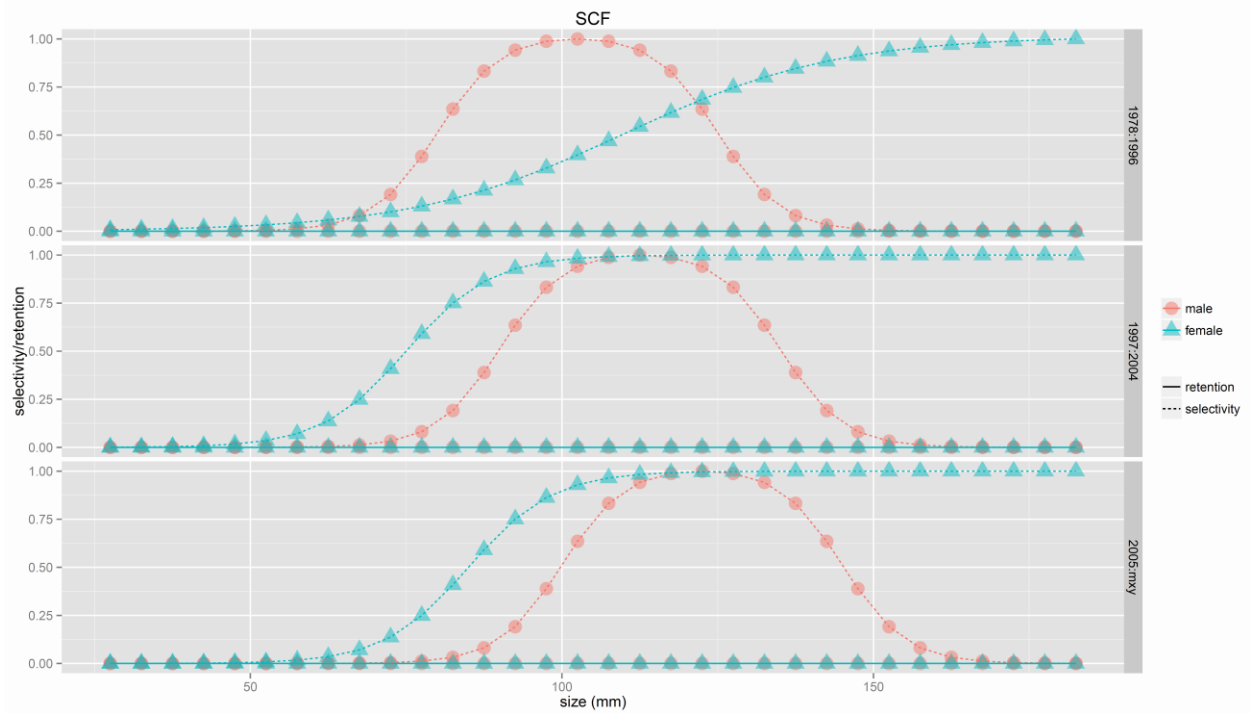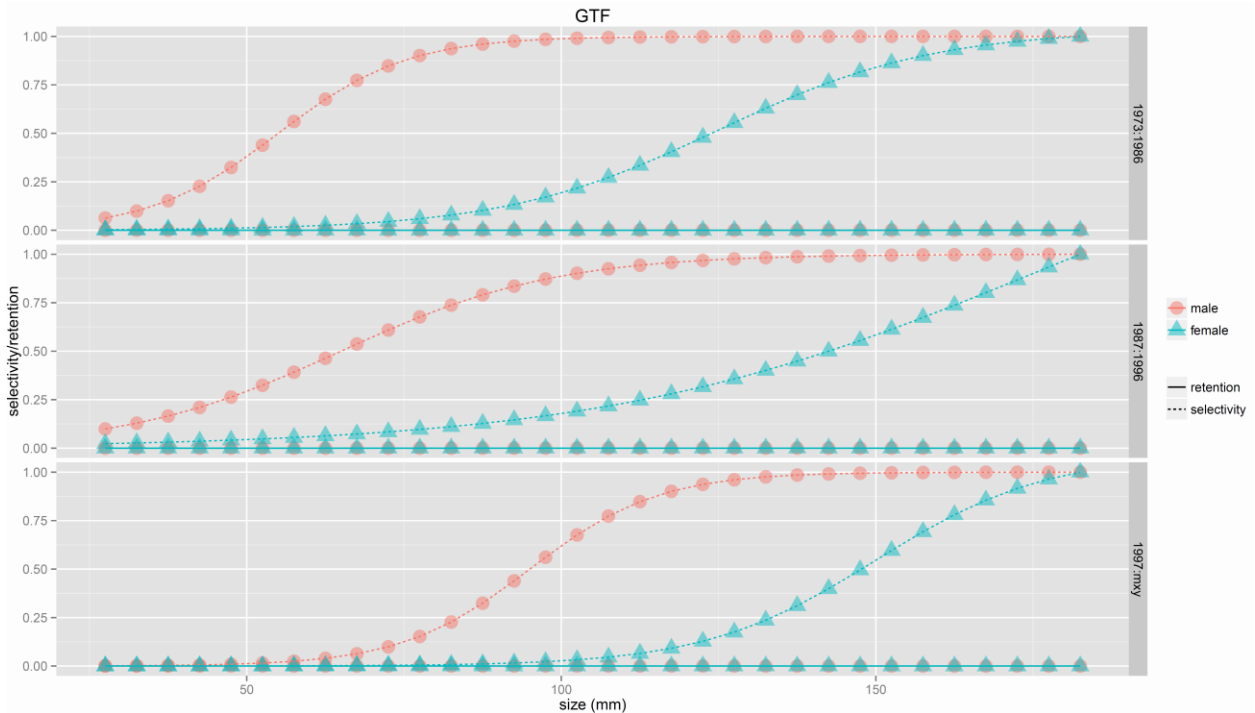

Fig. 6c.4. Selectivity and retention curves in three time blocks for the simulated crab bycatch fishery, SCF. Upper graph: 1978-1996. Center graph: 1997-2004. Lower graph: 2005-2013.
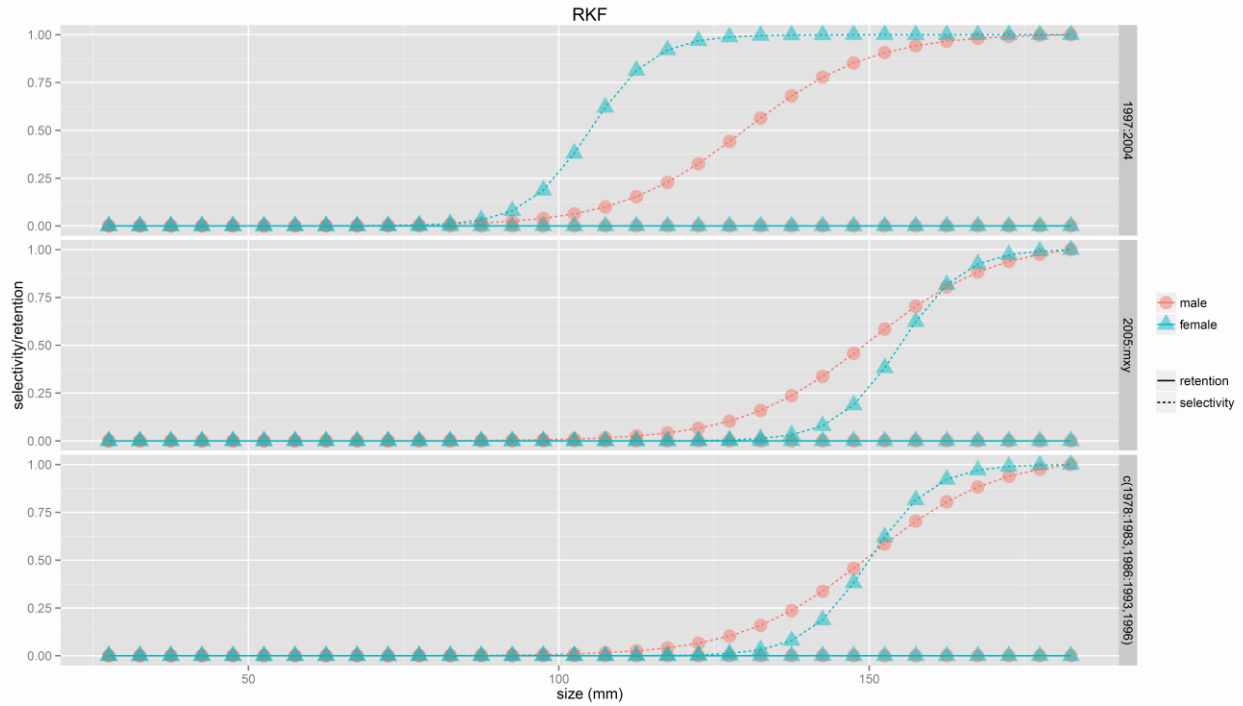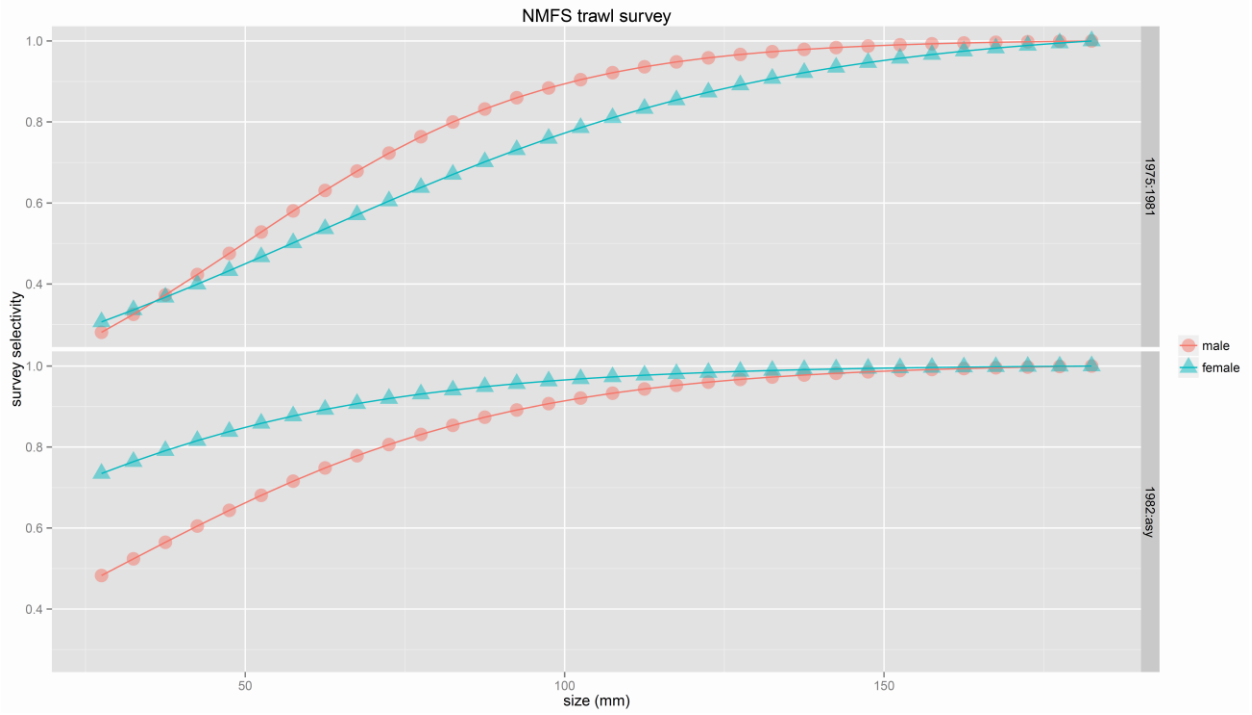
Fig. 6c.5. Selectivity and retention curves in three time blocks for the simulated crab bycatch fishery, RKF. Upper graph: 1997-2004. Center graph: 2005-2013. Lower graph: 1978-1996.

Fig. 6c.6. Selectivity and retention curves in three time blocks for the simulated trawl bycatch fishery, GTF. Upper graph: 1973-1986. Center graph: 1987-1996. Lower graph: 1997-2013.

Fig. 6c.7. Selectivity curves in two time blocks for the simulated NMFS trawl survey. Upper graph: 1975-1981. Lower graph: 1982-2014.
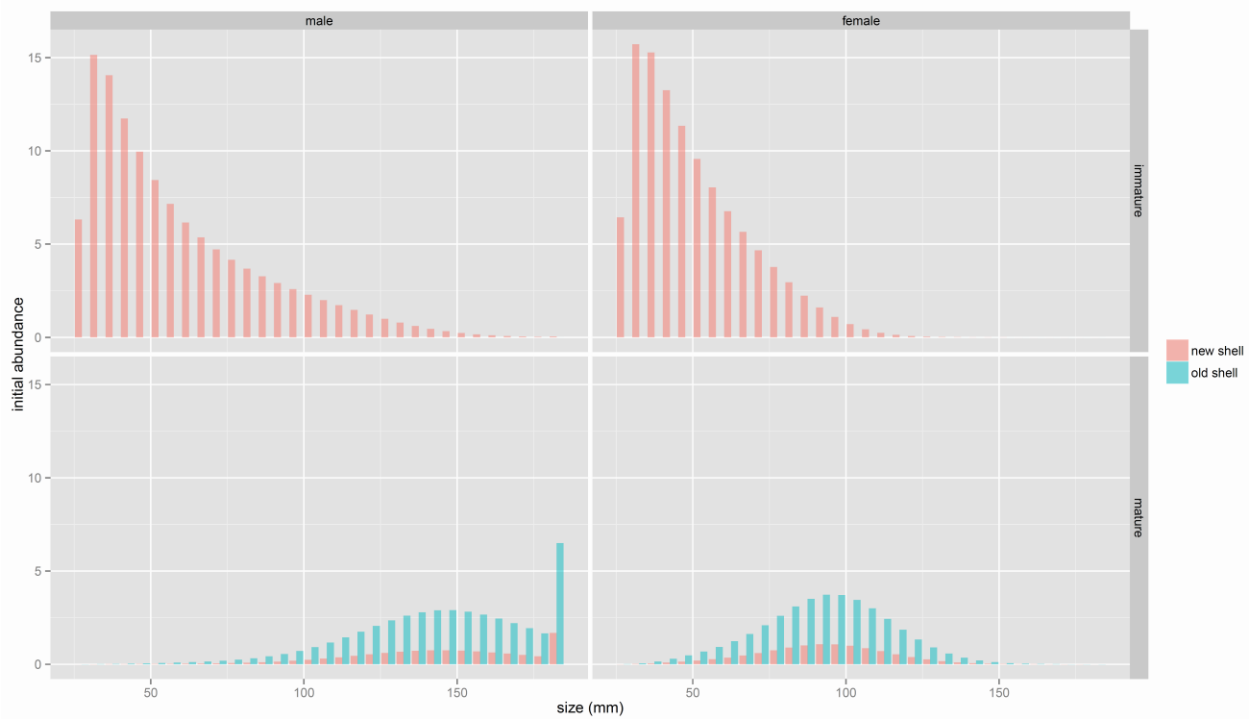
Fig. 6c.8. Initial size compositions, based on the equilibrium calculations outlined in Section 4.
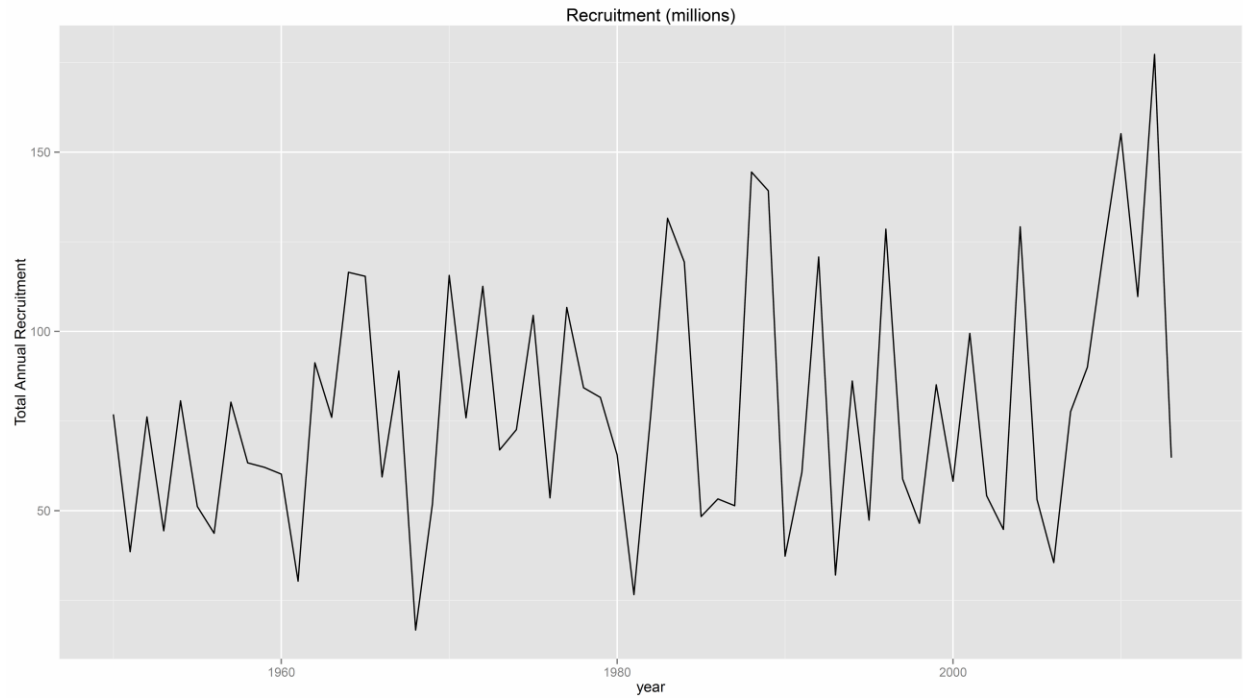
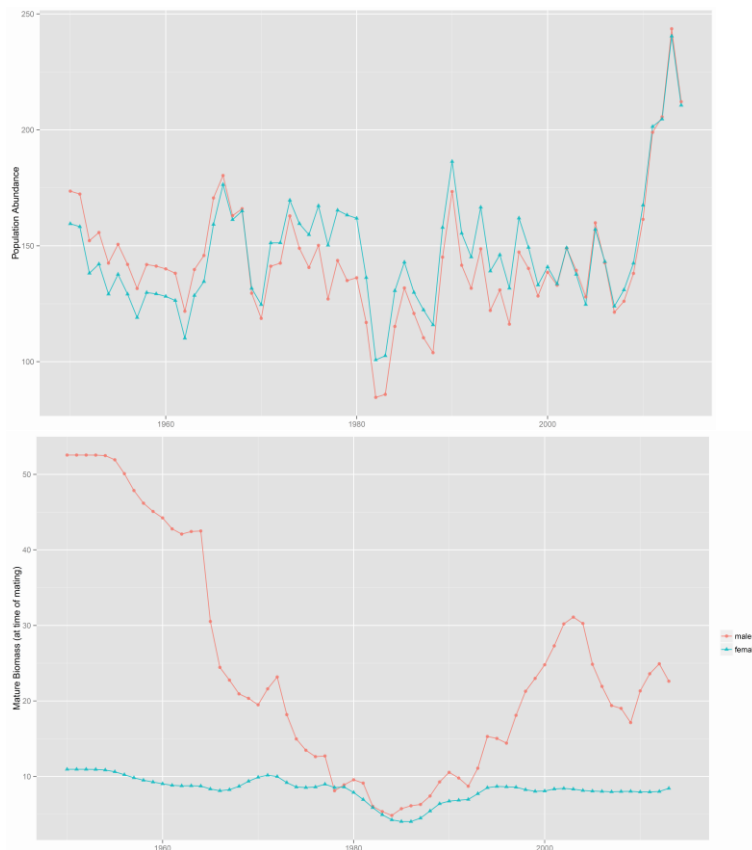Fig. 6c.9. Time series of simulated recruitment.

Fig. 6c.10. Time series of simulated population abundance (upper) and mature biomass (lower).
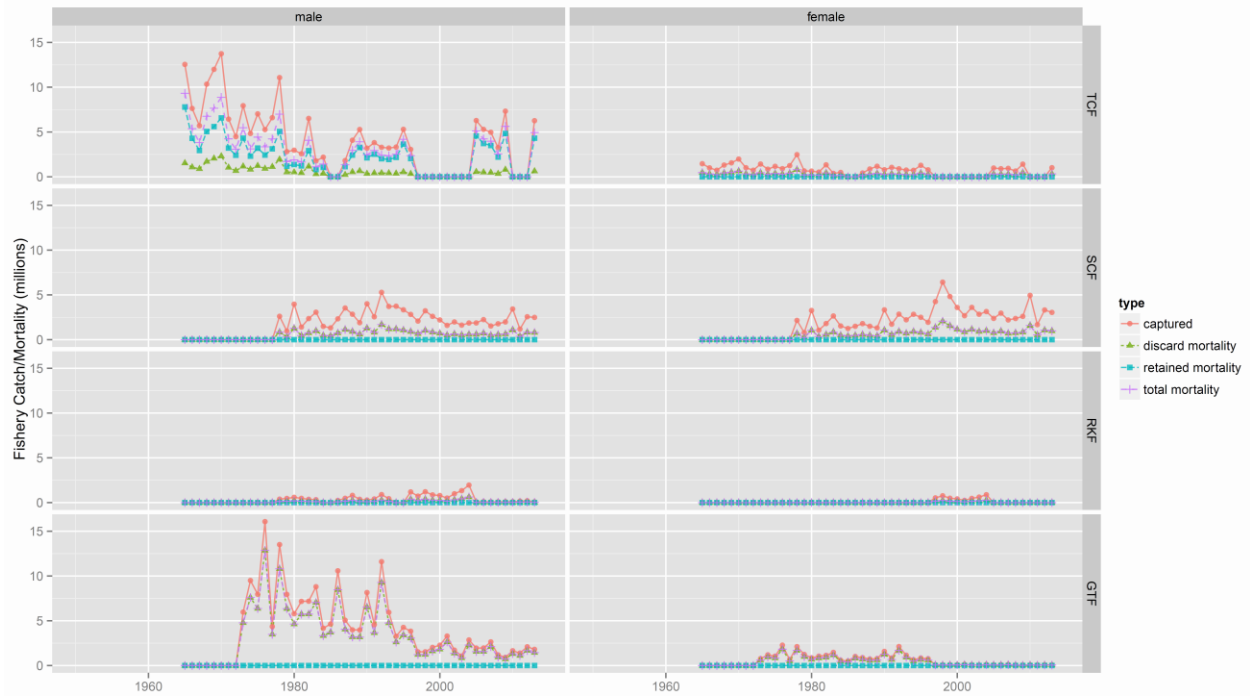
Fig. 6c.11. Time series of the simulated numbers of crab captured by the fisheries, as well as the mortality (numbers) associated with discards and retention.
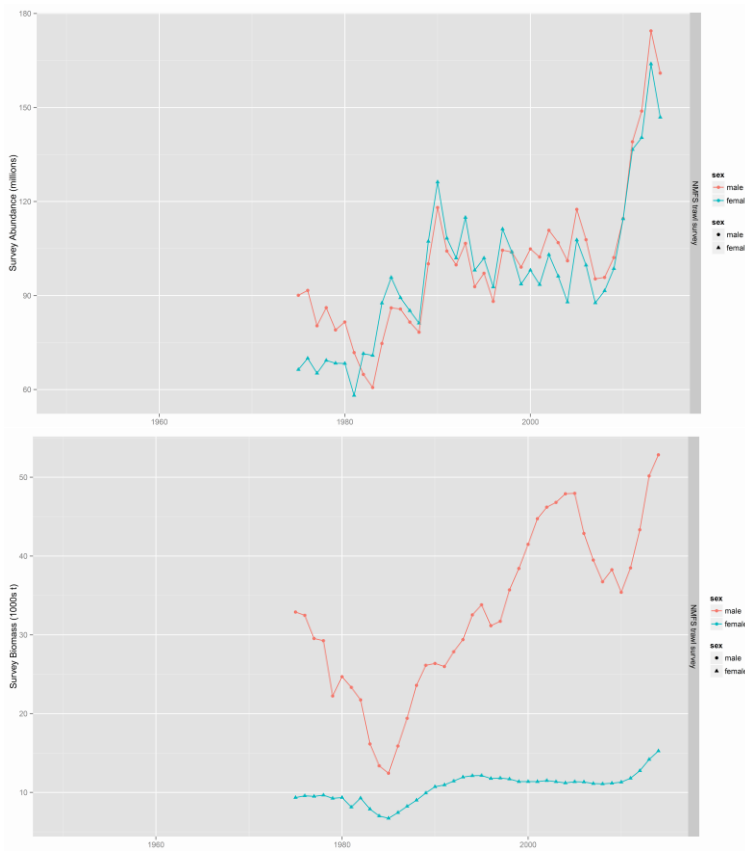

Fig. 6c.12. Time series of simulated survey abundance (upper plot) and biomass (lower plot).

6.d. A more complex simulated dataset: TCSAM2015 Results

I've run one TCSAM2015 model scenario, 'A2a', against the simulated A2 dataset described in the previous section. Parameters that were fixed in the model run were set to their corresponding values in the simulation (Table 6d.1). Time blocks defined in the simulation were also defined in the model configuration. Similarly, functional forms for all selectivity and retention functions defined in the simulation were also used in the model configuration. Median recruitment and ln-scale devs were estimated, but the sex ratio and size composition at recruitment were fixed. All ln-scale offsets to the (fixed) base rate of natural mortality were estimated (i.e., changes between time blocks, differences between males and females, differences between immature and mature crab, and differences between immature females and other crab; see the detailed description of natural mortality parameterization in Section 3B). All growth parameters were fixed. Parameters describing the probability of molting to maturity were estimated. Sex-specific ln-scale offsets to median fishery capture rates were fixed, but median capture rates, ln-scale annual deviations in capture rates, and parameters for (sex-specific) selectivity and retention functions were estimated. Median survey catchability (Q) was fixed, but ln-scale offsets were estimated for female catchability, as well as parameters for sex-specific selectivity functions.

Table 6d.1. TCSAM2015 model scenarios for dataset A2.

Process	Component	TCSAM2015 Model Scenario A2a
recruitment	median	estimated
	ln-scale devs	estimated
	sex ratio	fixed
	size composition	fixed
natural mortality	base	fixed
	offsets	estimated
growth		fixed
maturity		estimated
All fisheries	median F	estimated
	F offsets	fixed
	ln-scale devs	estimated
	male selectivity	estimated
	female selectivity	estimated
	retention	estimated
Survey	median Q	fixed
	Q offsets	estimated (female only)
	male selectivity	estimated
	female selectivity	estimated
initial size composition		0

For the simulated directed fishery (TCF), retained, discard, and total catch data were fit in the model for each sex and shell condition combination using lognormal likelihoods for abundance and biomass time series and multinomial likelihoods for size compositions. For the simulated crab bycatch fisheries (SCF, RKF), only total catch data were fit for each sex and shell condition combination, also using lognormal likelihoods for abundance and biomass time series and multinomial likelihoods for size compositions. Abundance and biomass time series were assigned error cv's of 5% and 10%, respectively, while size composition sample sizes were set to 50 per sex/shell condition combination. For the simulated groundfish bycatch fishery (GTF), only total catch data were fit—using lognormal likelihoods for abundance and biomass time series and multinomial likelihoods for size compositions, as well, but only by sex. All abundance and biomass time series were assigned error cv's of 5% and 10%, respectively,

while all size composition sample sizes were set to 50 per sex/shell condition (TCF, SCF, RKF) or per sex (GTF) combination.

For the simulated survey, survey catch data were fit in the model for each sex/maturity state/shell condition combination using lognormal likelihoods for the abundance and biomass time series and multinomial likelihoods for the size compositions. Abundance and biomass time series were assigned error cv's of 15% and 20%, respectively, while all size composition sample sizes were set to 25 for each sex/maturity state/shell condition combination.

The A2a model run converged and a valid hessian was obtained. Comprehensive plots of model results and model/simulation comparisons are available in the online material (files 'A2a.plots.tcsam.pdf' and 'A2.plots.comparison.pdf'). The ability of the TCSAM2015 model to fit the simulated data in this more complex scenario appeared, as with the simpler A1 scenario discussed previously, to be excellent (Fig.s 6d.1-18). Objective function values for the various data components were small for all four fisheries, as well for the survey (Fig.s 6d.1-3). The "worst" fits were obtained for immature crab size compositions in the survey (Fig. 6d.3), although these were really still quite small. Examining the model fits to the different data sources visually reinforces that the model did quite well in fitting the simulated data, as one would expect (e.g., Fig.s: 6d.4, survey abundance; 6d.6, survey biomass; 6d.9, TCF total catch abundance; 6d.11 TCF total catch biomass; 6d.14, SCF total catch abundance; 6d.16, SCF total catch biomass; see the online material for fits to size compositions and for plots for RKF and GTF data sources).

Although all z-scores and residuals were quite small (e.g., Fig.s: 6d.5, survey catch abundance; 6d.7, survey catch biomass; 6d.8 survey size compositions), two patterns were notable. First, z-scores for female survey biomass between 1975 and 1981 (the first survey selectivity time block) were biased slightly positive for mature crab and negative for immature crab (Fig. 6d.7). Second, female survey size compositions during this time block exhibited much larger patterned residuals than in the second time block (Fig. 6d.8). A slight patterning associated with the different fishery selectivity time blocks was also evident in the residuals for SCF total catch size compositions.

Natural mortality rates appear to have been estimated quite well for mature crab, but underestimated for immature crab (Fig. 6d.19). As discussed in detail in Section 3, natural mortality is parameterized using ln-scale parameter offsets to a base mortality rate for mature males. Parameter uncertainty, as reflected by the estimated standard deviation, for the ln-scale temporal shift in natural mortality during the simulated 1980-1984 "high mortality" period (pLnDMT[1]) and ln-scale offsets for female crab in both the high mortality period (pLnDMX[2]) and the remainder (pLnDMX[1]) was small (cv's ~3%; Fig. 6d.20). Parameter uncertainty was higher for ln-scale offsets for immature crab (cv's ~10%).

The shapes of the logistic curves used to simulate the probability of immature crab molting to maturity were well-estimated by the model (Fig. 6d.21). The agreement is particularly good considering that the model is not fitting a logistic function to the data, but is instead using a set of a set of parameters, one per size bin (by sex), and two constraints (non-descending and smooth functions) to describe the probability functions.

Of the selectivity curves used to simulate the data (Fig.s 6d.22-26), only those used to simulate the survey data (Fig. 6d.22) were not terribly well-estimated by the model, but this may be due to a lack of contrast

in the survey selectivity functions over the simulated size ranges. The simulated selectivity curves (based on the assessment model) are quite flat, with the greatest difference occurring between the curves for females in the 1975-1981 time block. In addition, fully-selected survey catchability ("Q") for females is substantially underestimated for this time block (Fig. 6d.27), although differences in size-averaged Q (which take into account both the fully-selected Q and the shape of the selectivity curve, Fig. 6d.28) are much smaller. These mismatches appear to be the main driver for the distinct patterns in residuals noted for females in the survey (Fig.s 6d.7-8).

The various fishing rates (fully-selected and size-averaged) estimated by the model agree exceedingly well with those from the simulation (e.g., Fig.s 6d.29-30 for TCF, see the online material for the others), to the extent that it appears that only the model estimates are plotted.

The TCSAM2015 model follows the overall temporal pattern of simulated ("true") annual recruitment subsequent to 1960 quite well, but almost consistently underestimates the true number of recruits. Not surprisingly, this pattern is also apparent in the time series of estimated vs. true population abundance. However, the difference disappears for the mature biomass time series following a "model startup" period prior to 1965 when the model is uninformed by any data and building up its population through recruitment. These patterns probably result from tradeoffs between estimating natural mortality and recruitment levels. Because agreement was quite could for mature biomass after the startup period, the model was estimating numbers of mature crab well—as it had to in order to fit both fishery catch abundance and biomass trends and survey biomass trends as well as it did. The model estimated natural mortality (and fishing mortality) well for mature crab. It did, however, underestimate natural mortality on immature crab (Fig. 6d.19), which would tend to make it also underestimate recruitment in order to achieve similar numbers and biomass of mature crab. Because the principal information on recruitment comes through survey data for the model, this suggests that (in this case) weighting the survey data more equally with the fisheries data might have resulted in better estimates of natural mortality on immature crab and on mean recruitment.

Finally, I've plotted the ratio of annual total discard biomass mortality (i.e., summed over all crab) to annual total discard biomass in Fig. 6d.34. The ratios for all fisheries for both the simulation and the model agree with the discard mortality rates used in both, providing a check on the consistency of the Gmacs-style fishing mortality equations in a multiple-fishery scenario.
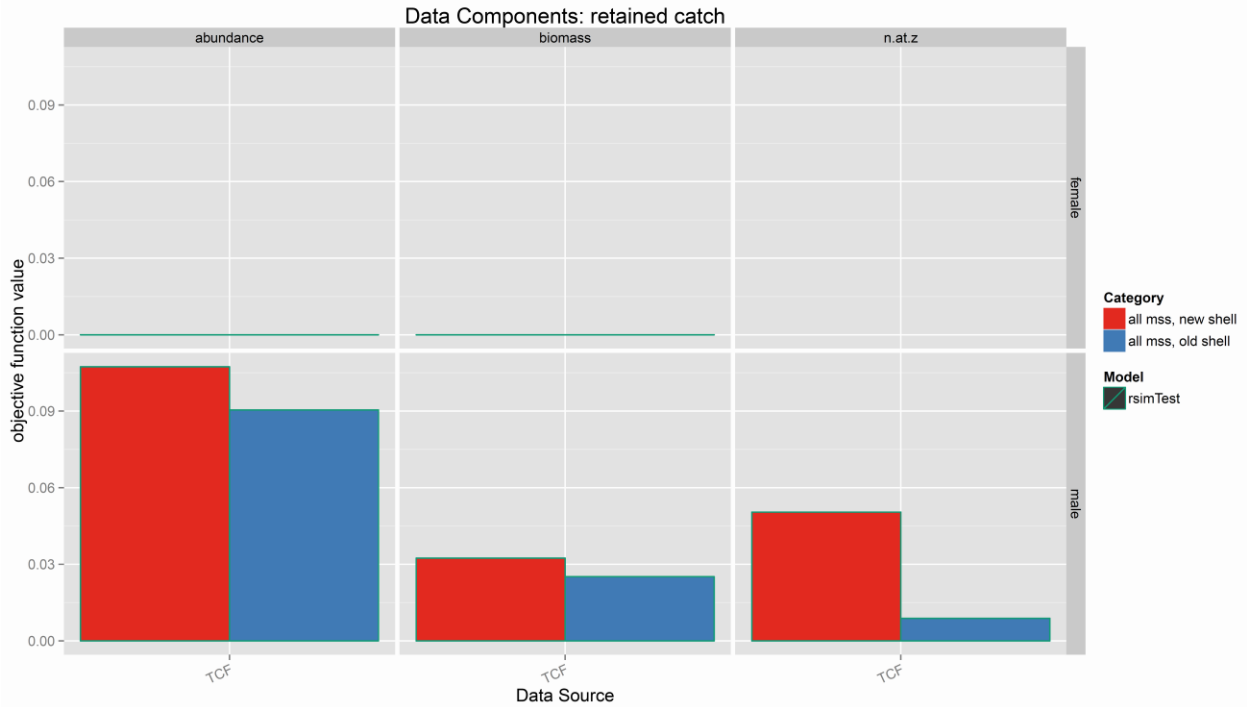
Fig. 6d.1. Objective function values for the simulated directed fishery (TCF) obtained by fitting retained catch abundance, biomass, and size compositions ("n.at.z"). No female crab were retained. "all mss" denotes all maturity states. "rsimTest" denotes the TCSAM2015 model A2a.
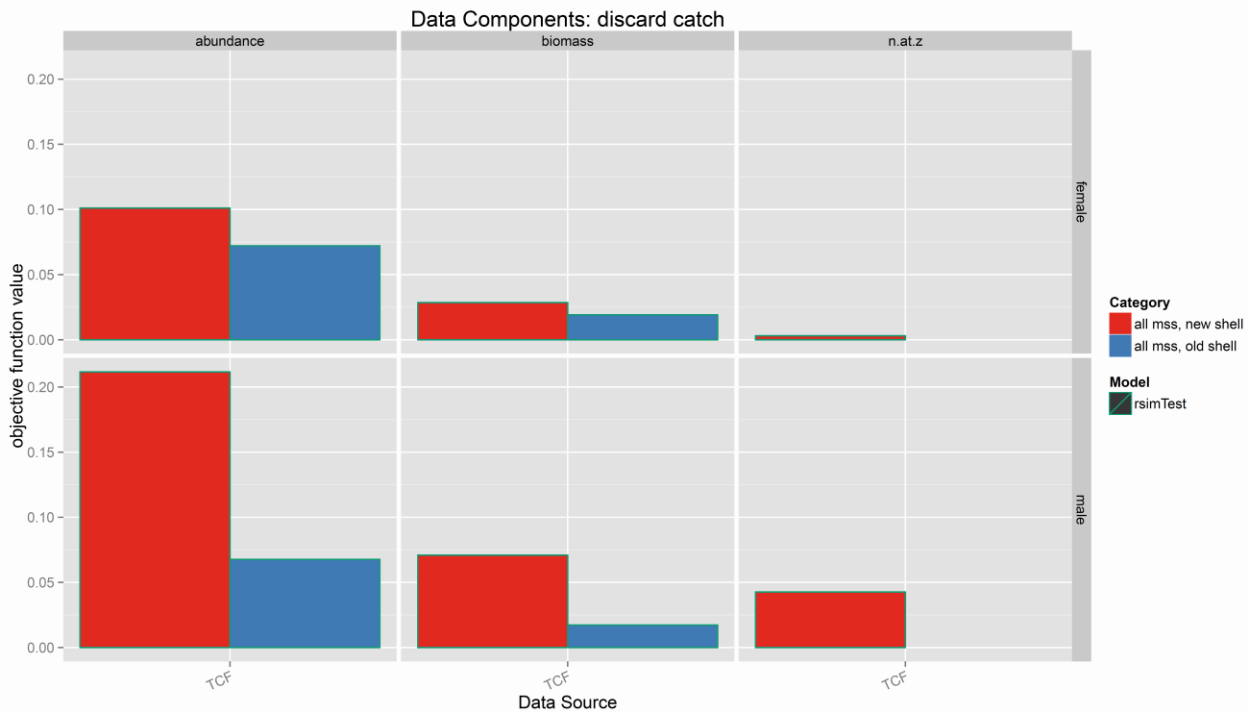

Fig. 6d.2. Objective function values for TCF obtained by fitting discarded catch abundance, biomass, and size compositions ("n.at.z"). "all mss" denotes all maturity states. "rsimTest" denotes the TCSAM2015 model A2a.
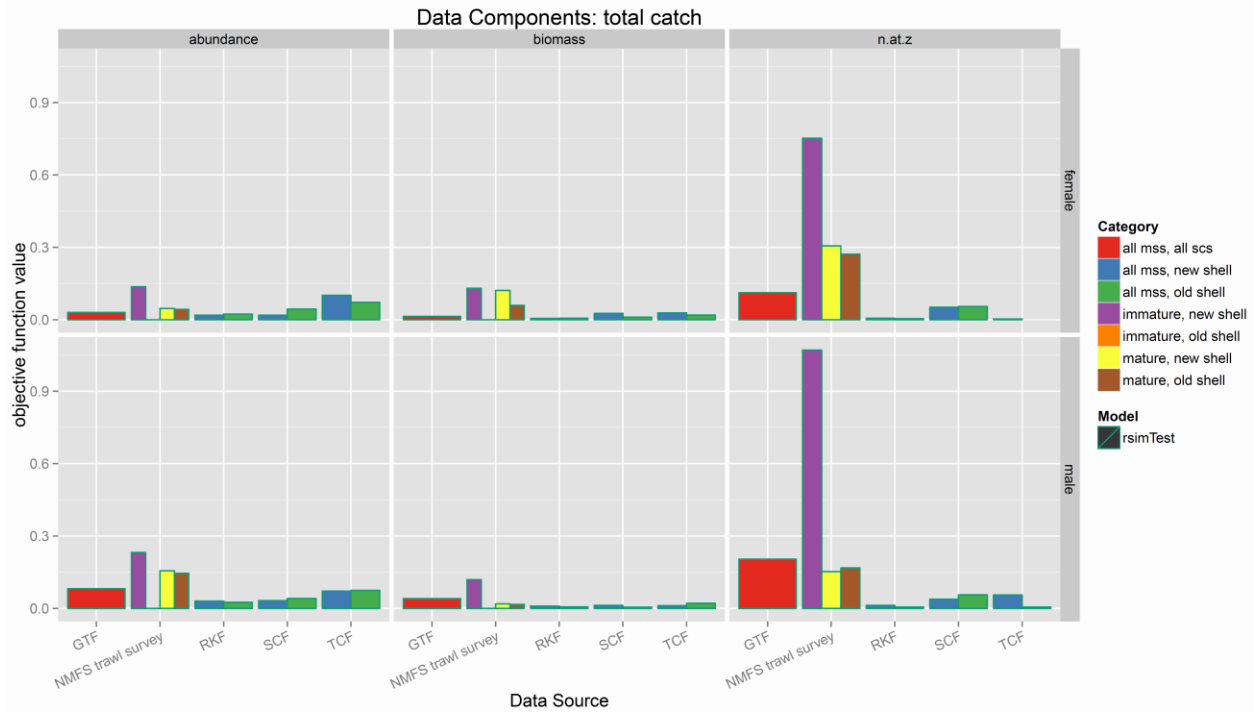
Fig. 6d.3. Objective function values for the four fisheries and the survey obtained by fitting total catch abundance, biomass, and size compositions ("n.at.z"). "all mss" denotes all maturity states, "all scs" denotes all shell conditions. "rsimTest" denotes the TCSAM2015 model A2a.
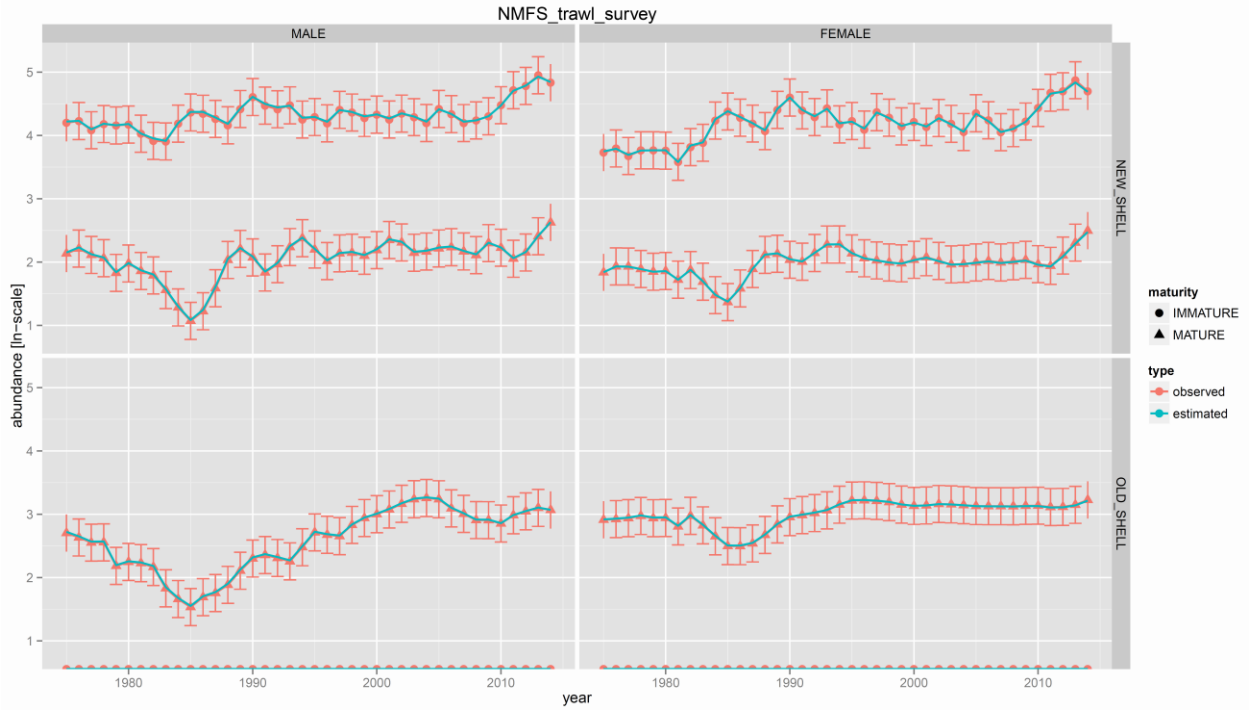
Fig. 6d.4. Fits to (ln-scale) simulated survey catch abundance.
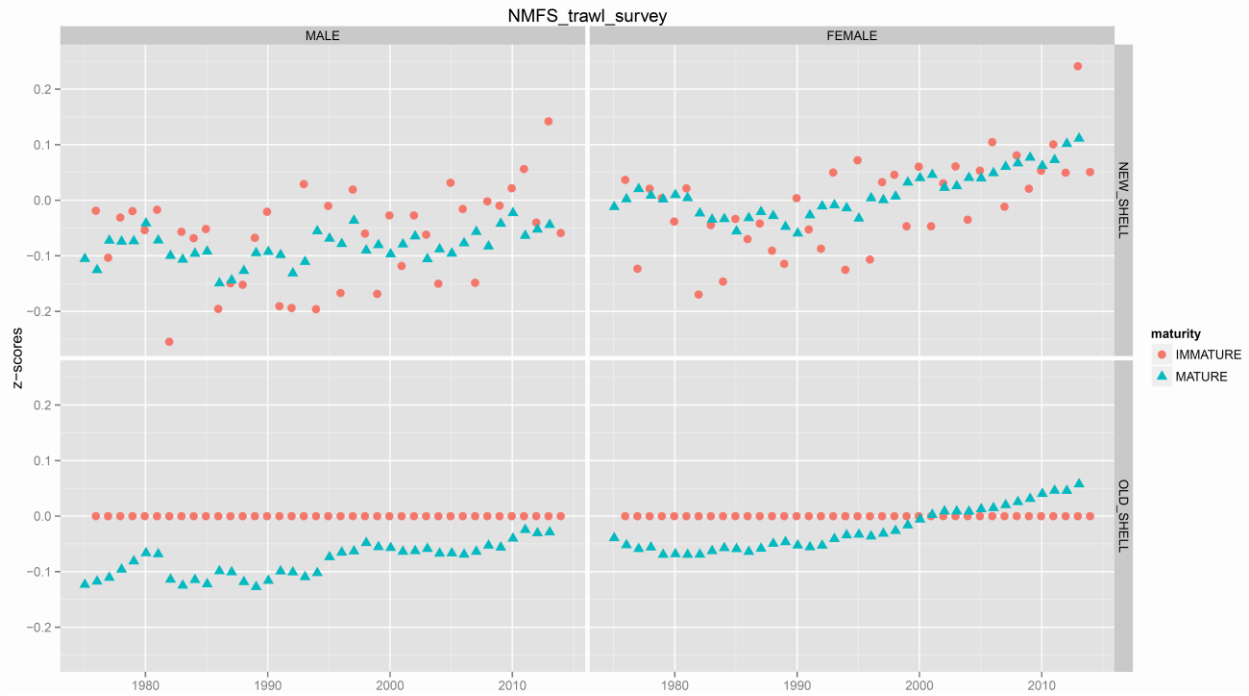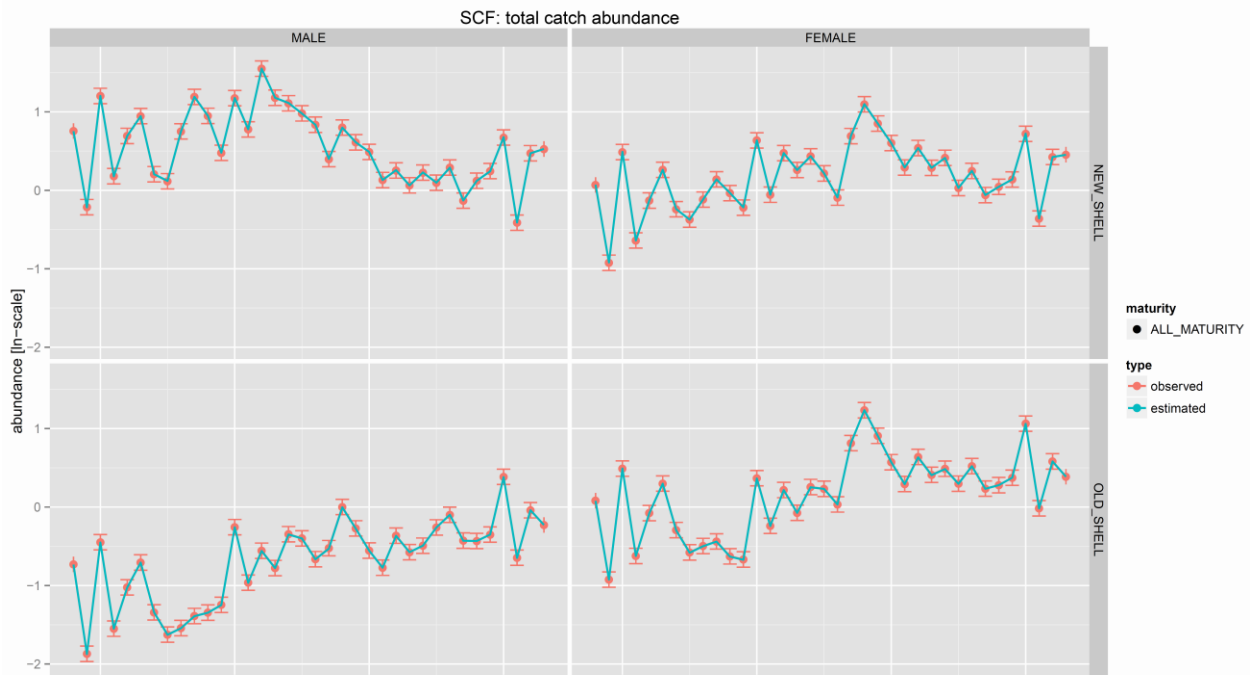

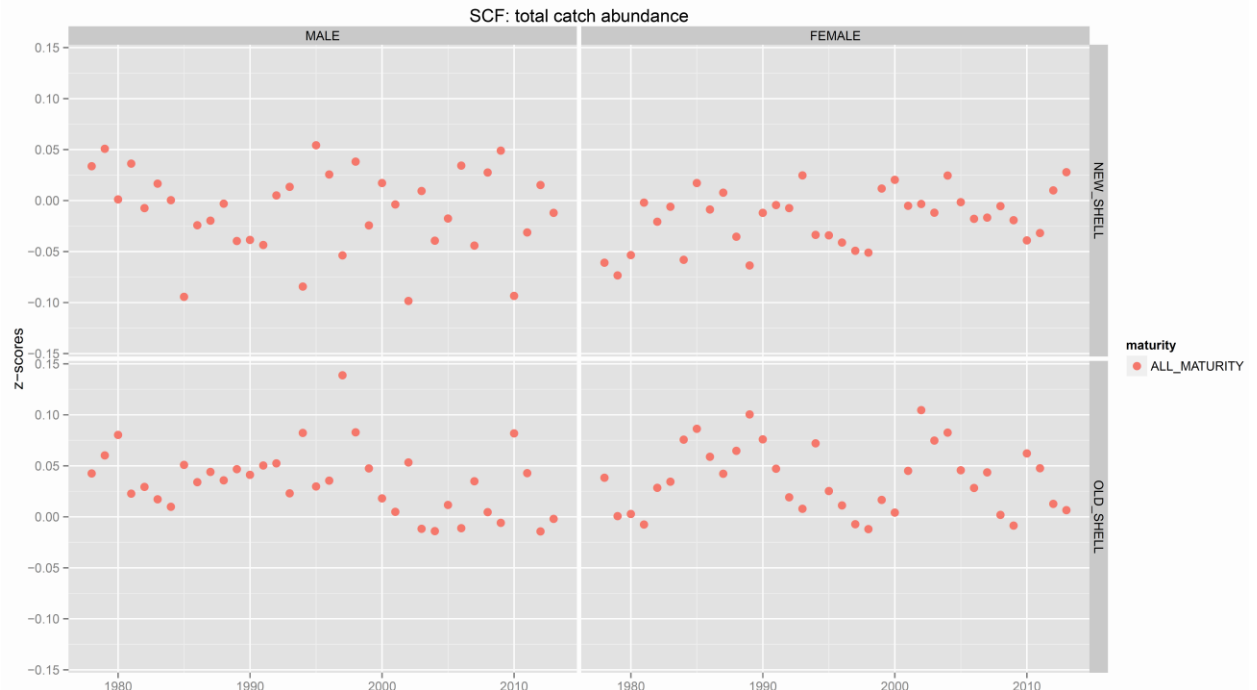
Fig. 6d.5. Z-scores for fits to simulated survey catch abundance.
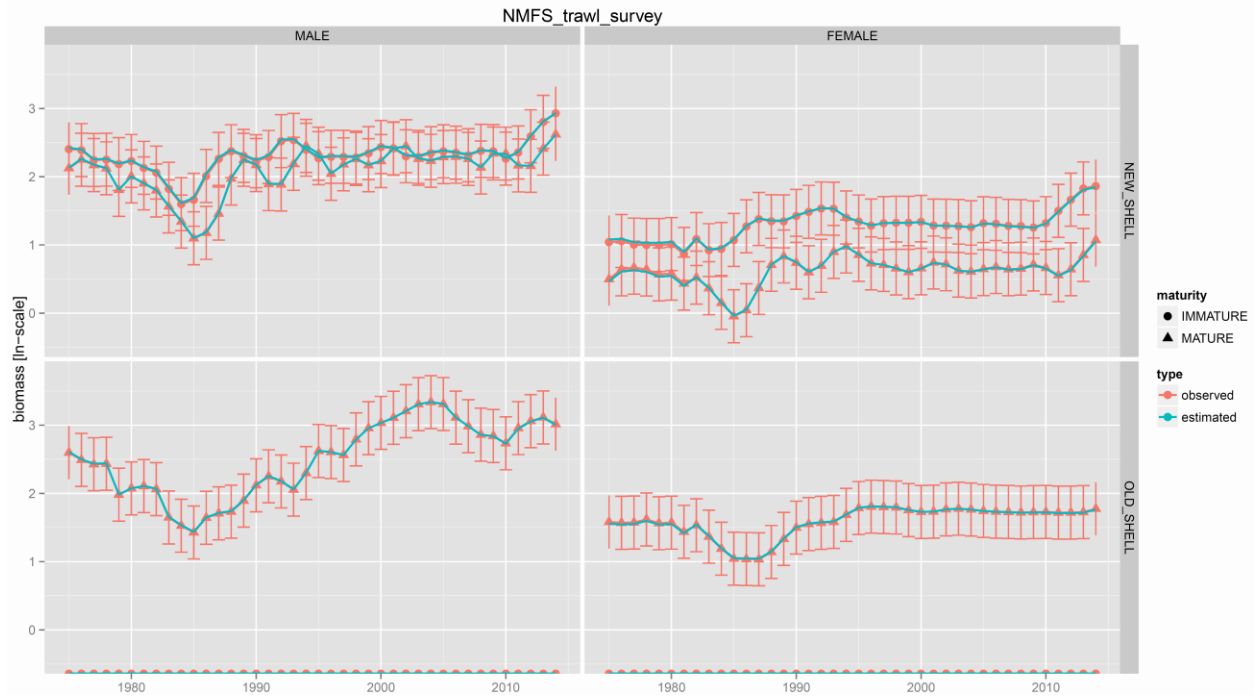
Fig. 6d.6. Fits to (ln-scale) simulated survey catch biomass.
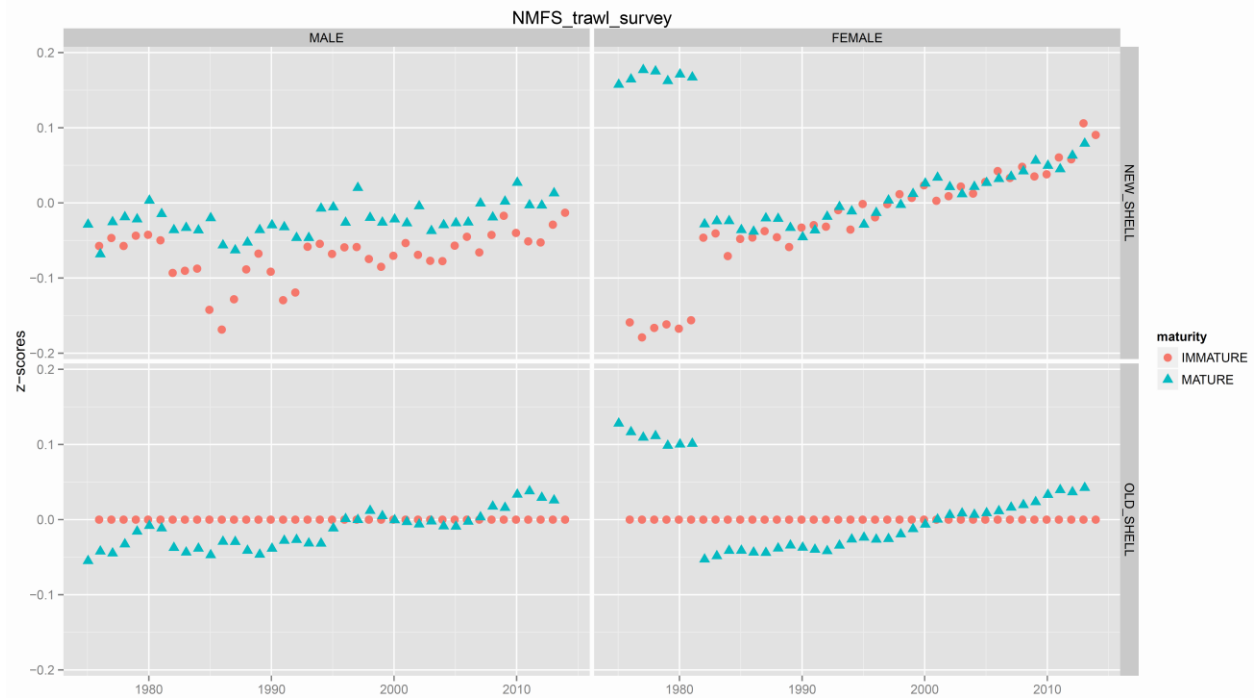
Fig. 6d.7. Z-scores for fits to simulated survey catch biomass.
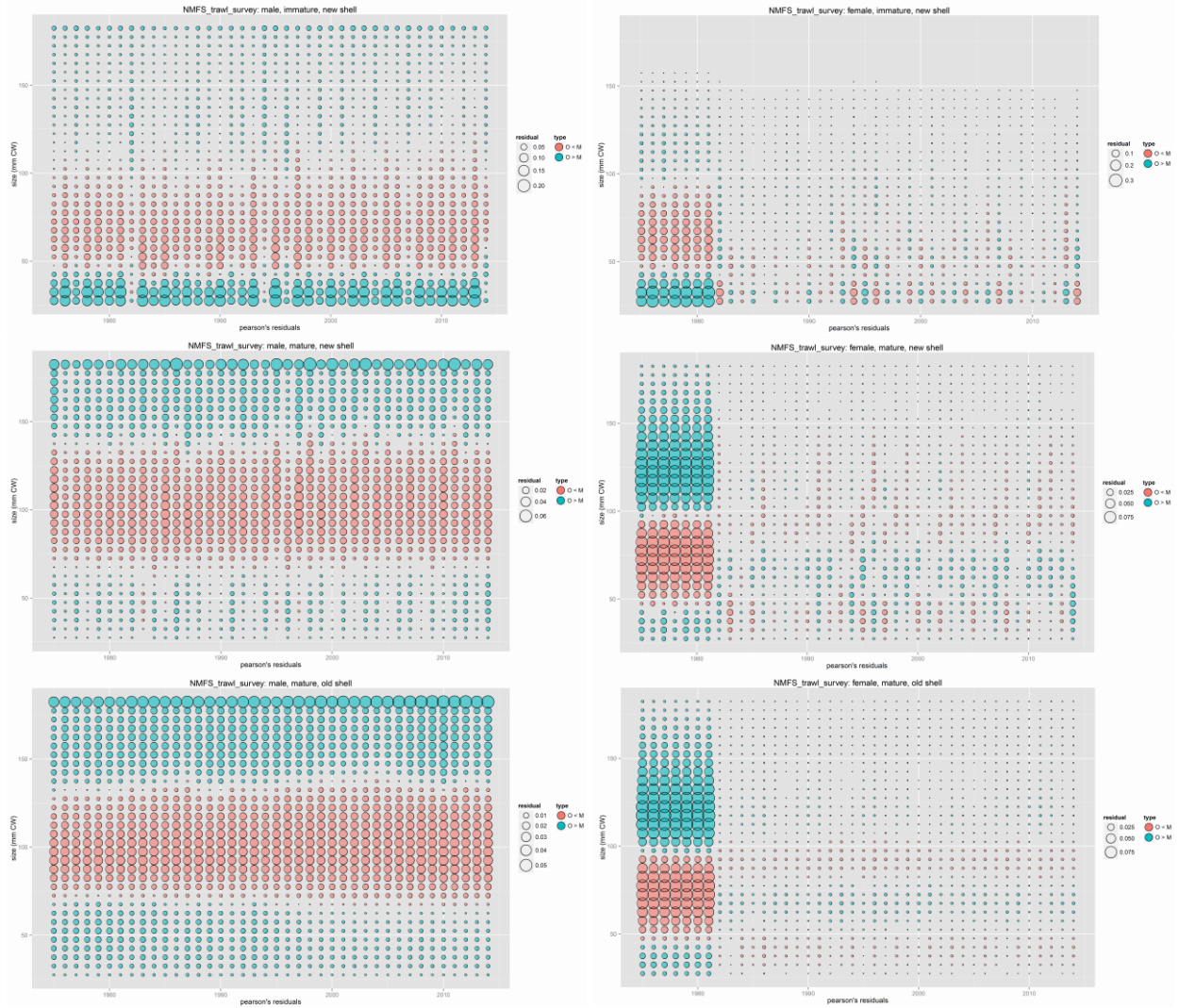
Fig. 6d.8. Pearson's residuals for fits to simulated survey size compositions by sex, maturity state, and shell condition. Left column: males; right column: females. Top row: immature, new shell crab. Center row: mature, new shell crab. Bottom row: mature, old shell crab. Turquoise: observed > estimated. Coral: observed < estimated. Max scales: 0.20, immature males; 0.3, immature females; 0.06, mature new shell males; 0.075, mature new shell females; 0.05, mature old shell males; 0.075, mature old shell females.

Fig. 6d.9. Fits to (ln-scale) simulated TCF total catch abundance.
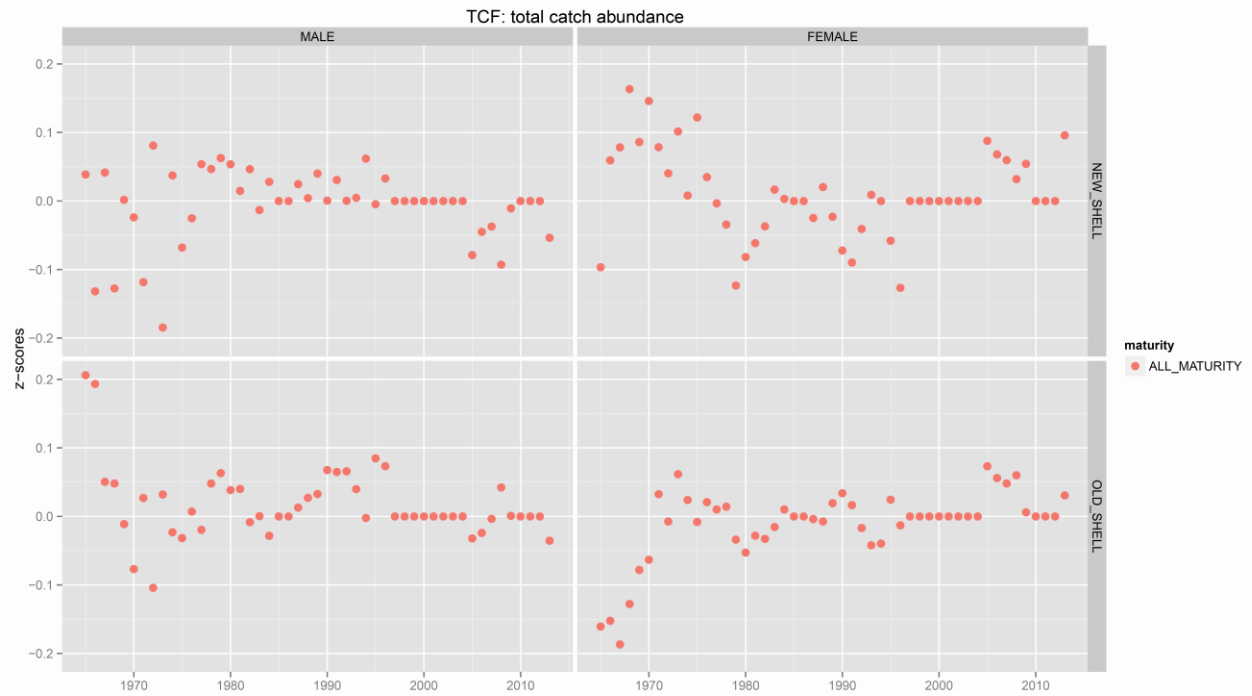
Fig. 6d.10. Z-scores for fits to simulated TCF total catch abundance.
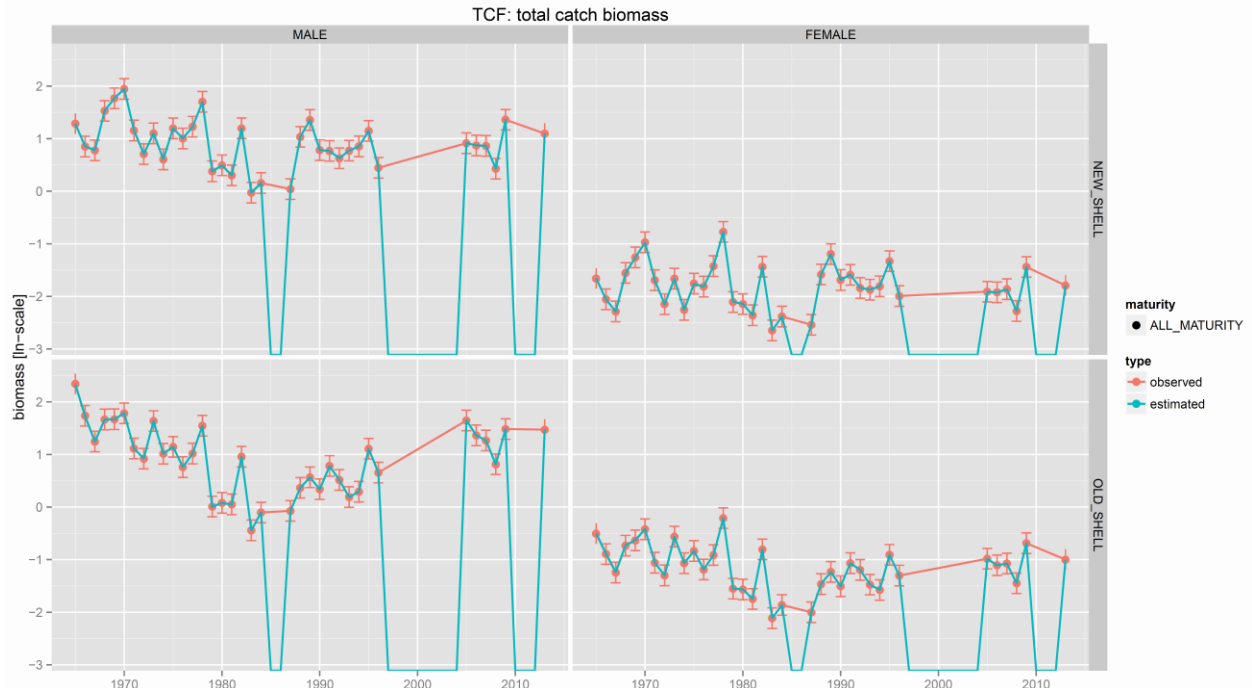
Fig. 6d.11. Fits to (ln-scale) simulated TCF total catch biomass.
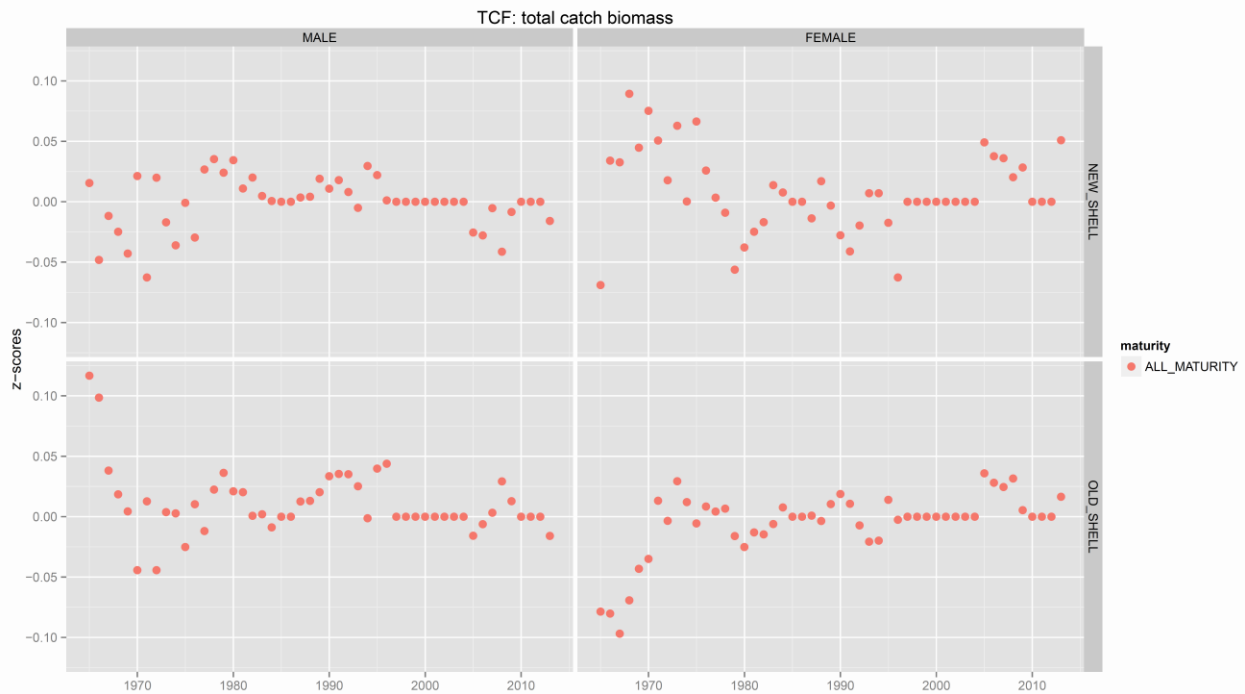
Fig. 6d.12. Z-scores for fits to simulated TCF total catch biomass.
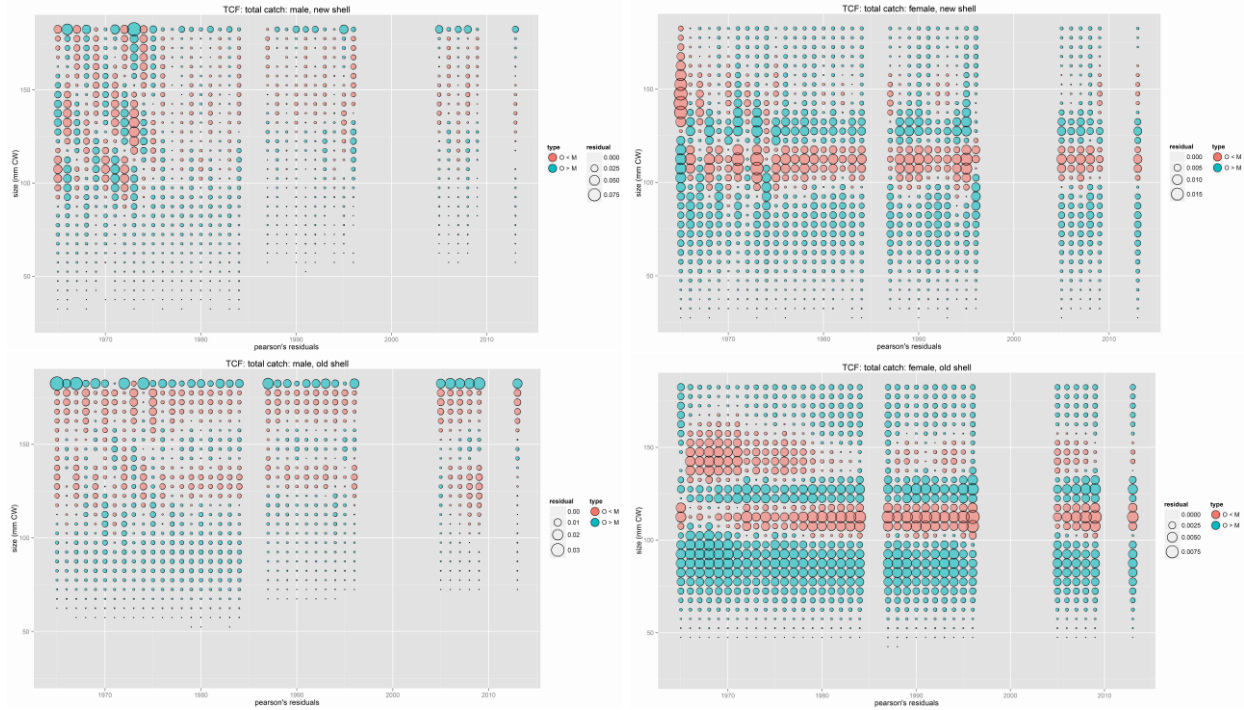
Fig. 6d.13. Pearson's residuals for fits to simulated TCF total catch size compositions by sex and shell condition. Left: males; right: females. Top: new shell crab. Bottom: old shell crab. Turquoise: observed > estimated. Coral: observed < estimated. Max scales: 0.075, new shell males; 0.015, new shell females; 0.03, old shell males; 0.0075, mature old shell females.

Fig. 6d.14. Fits to (ln-scale) simulated SCF total catch abundance.

Fig. 6d.15. Z-scores for fits to simulated SCF total catch abundance.

Fig. 6d.16. Fits to (ln-scale) simulated SCF total catch biomass.

Fig. 6d.17. Z-scores for fits to simulated SCF total catch biomass.
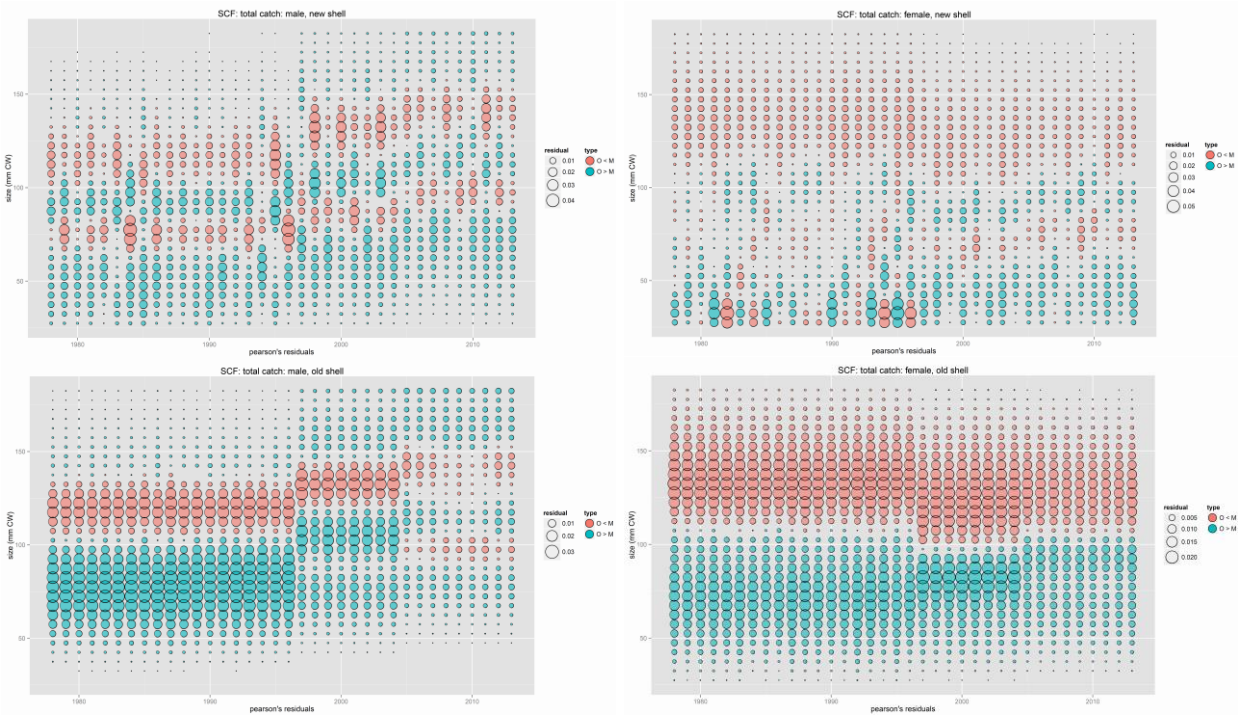
Fig. 6d.18. Pearson's residuals for fits to simulated SCF total catch size compositions by sex and shell condition. Left: males; right: females. Top: new shell crab. Bottom: old shell crab. Turquoise: observed > estimated. Coral: observed < estimated. Max scales: 0.04, new shell males; 0.05, new shell females; 0.03, old shell males; 0.02, mature old shell females.
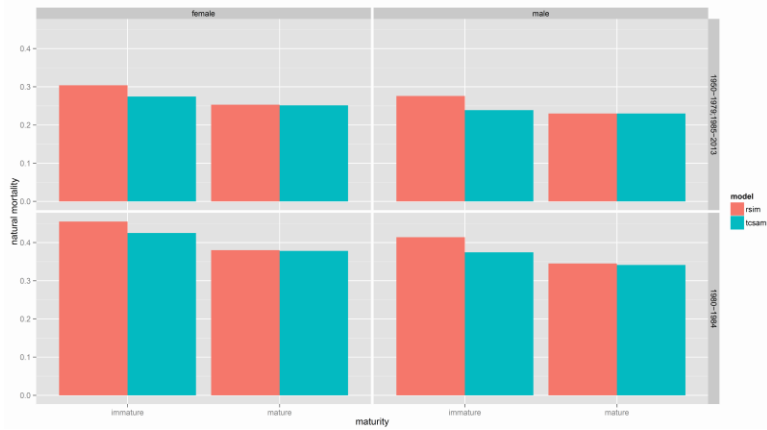
Fig. 6d.19. Comparison of estimated ("tcsam") and true ("rsim") natural mortality rates.
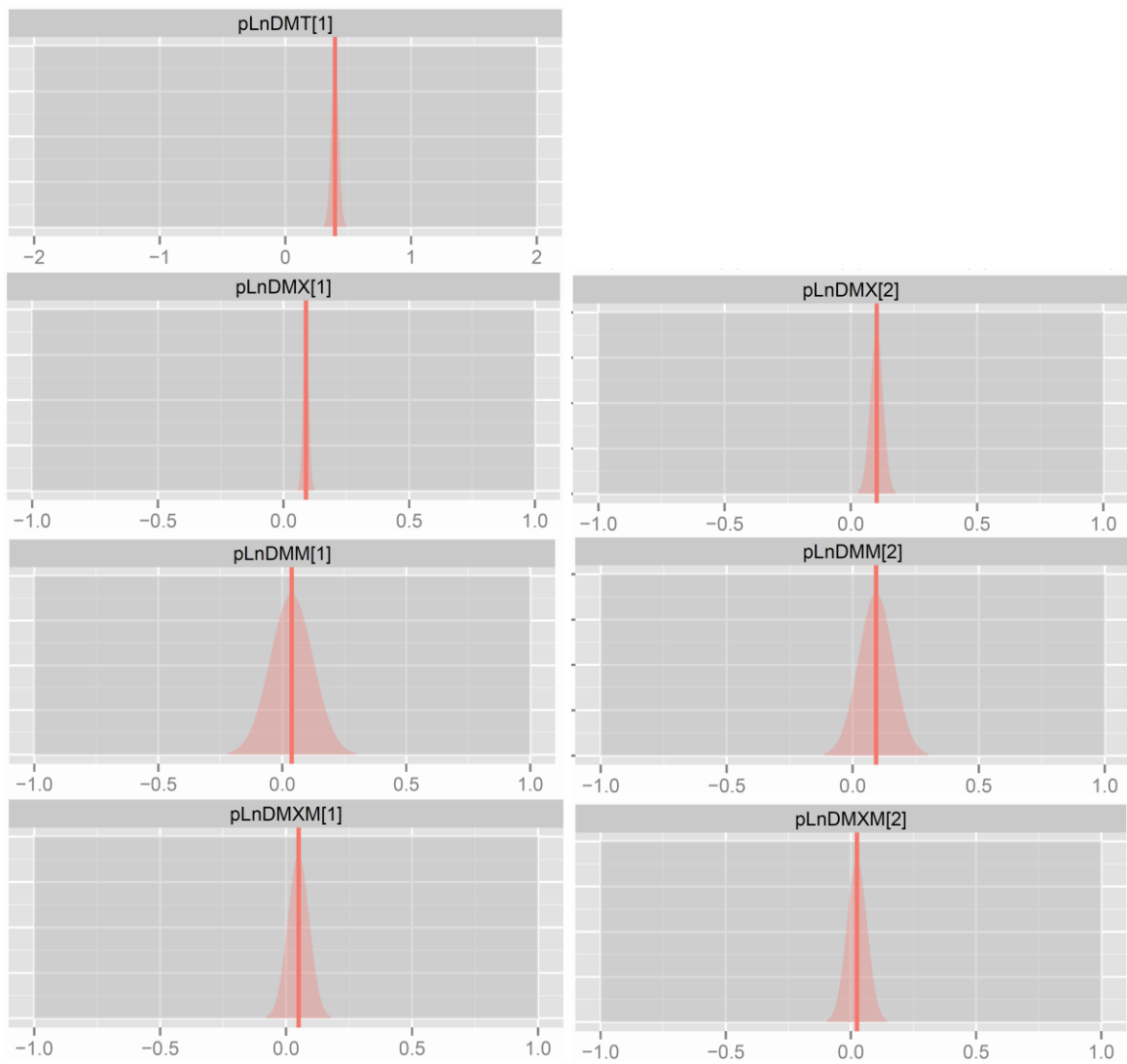
Fig. 6d.20. Estimates (vertical lines) and uncertainty (based on parameter standard deviations) in ln-scale parameter values related to natural mortality rates. See text for detail.
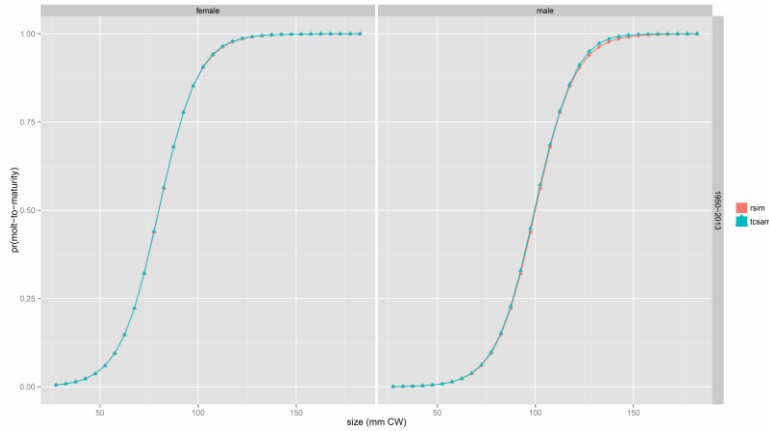
Fig. 6d.21. Comparison of estimated ("tcsam") and true ("rsim") size-specific molt-to-maturity probabilities. Left: females. Right: males.
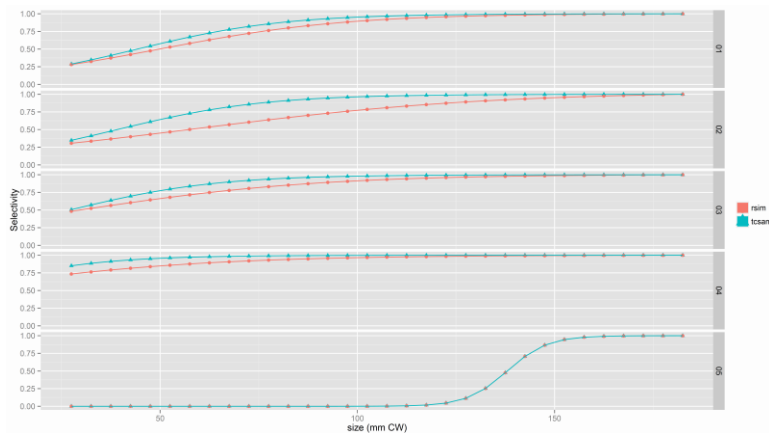
Fig. 6d.22. Comparison of estimated ("tcsam") and true ("rsim") selectivity functions. 01: survey males, 1975-81; 02: survey females, 1975-81; 03: survey males, 1982-2014; 04: survey females, 1982-2014; 05: male retention in TCF, 1965-2013.
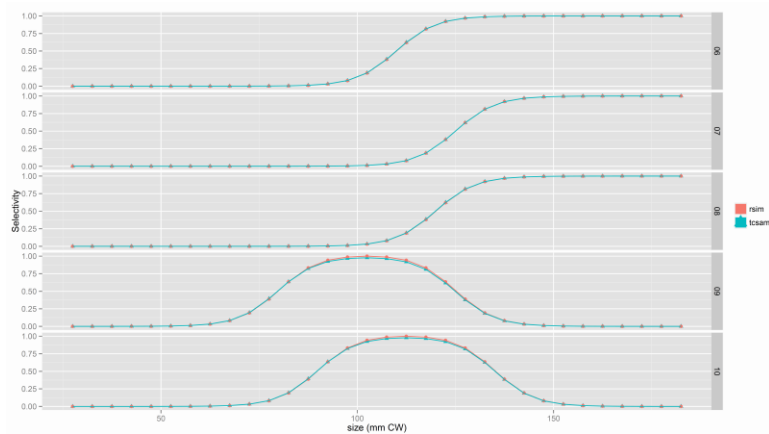
Fig. 6d.23.. Comparison of estimated ("tcsam") and true ("rsim") selectivity functions. 06: TCF males, 1965-84; 07: TCF males, 1987-2013; 08: TCF females, entire period; 09: SCF males, 1978-96; 10: SCF males; 1997-2004.
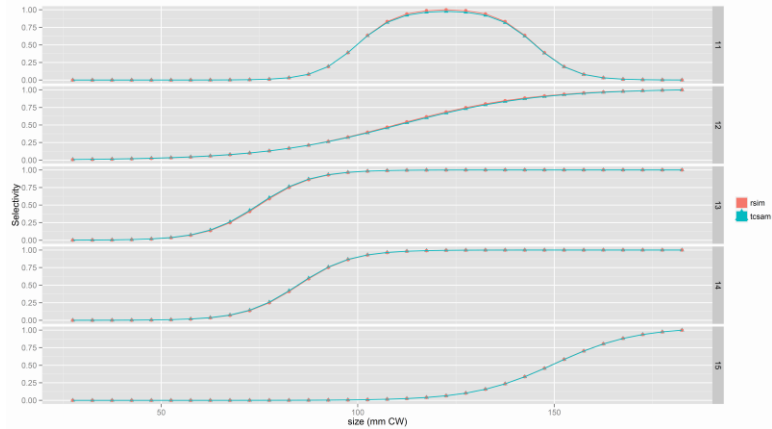
Fig. 6d.24. Comparison of estimated ("tcsam") and true ("rsim") selectivity functions. 11: SCF males, 2005-2013; 12: SCF females, 1978-1996; 13: SCF females, 1997-2004; 14: SCF females, 2005-2013; 15: RKF males; 1978-1996.
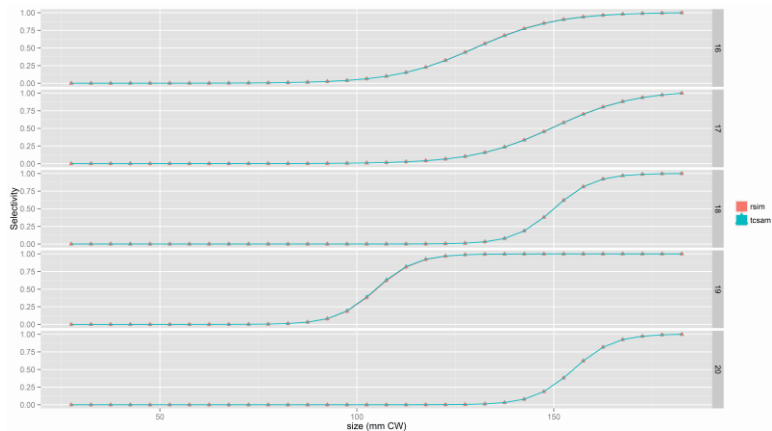
Fig. 6d.25. Comparison of estimated ("tcsam") and true ("rsim") selectivity functions. 16: RKF males, 1997-2004; 17: RKF males, 2005-2013; 18: RKF females, 1978-1996; 19: RKF females, 1997-2004; 20: RKF females; 2005-2013.
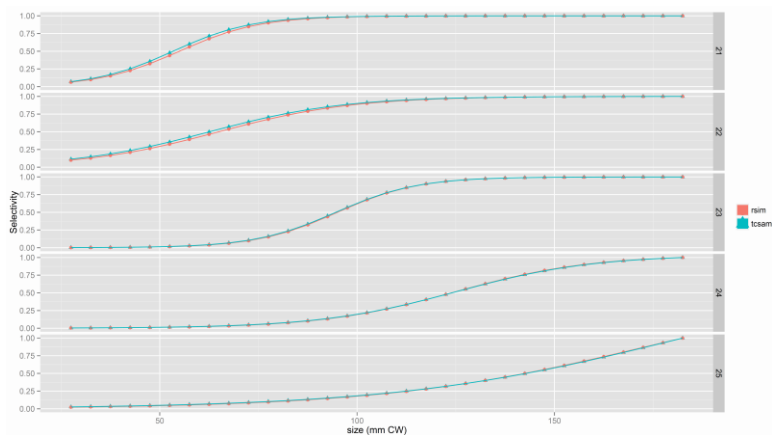

Fig. 6d.26. Comparison of estimated ("tcsam") and true ("rsim") selectivity functions. 21: GTF males, 1973-1986; 22: GTF males, 1986-1996; 23: GTF males, 1997-2013; 24: GTF females, 1973-1986; 25: RKF males; 1987-1996. [Note: GTF females, 1997-2013, not shown.]
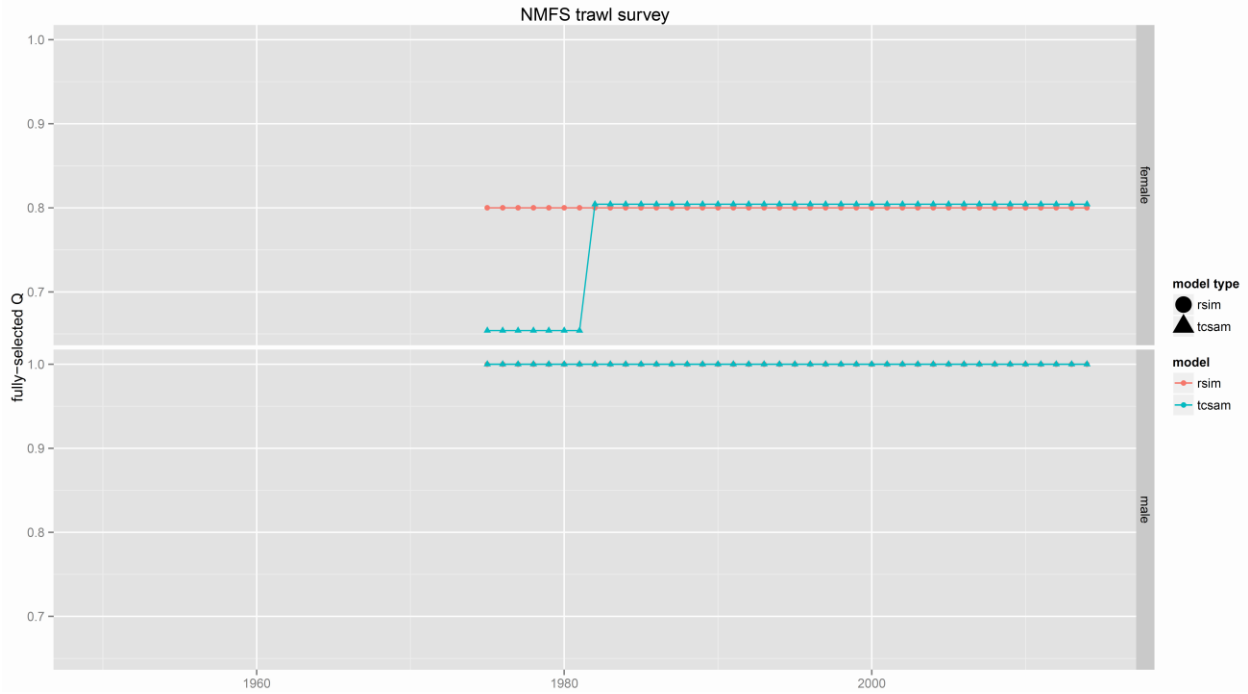
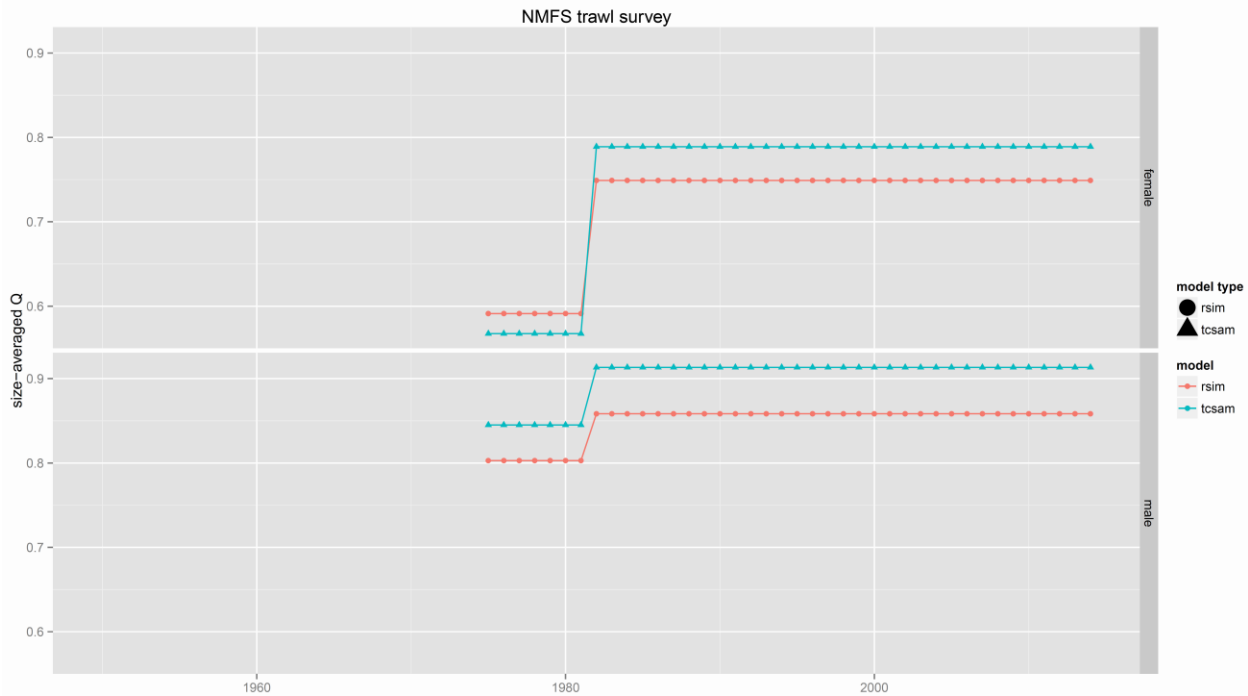Fig. 6d.27. Comparison of estimated ("tcsam") and true ("rsim") fully-selected annual survey Q's.

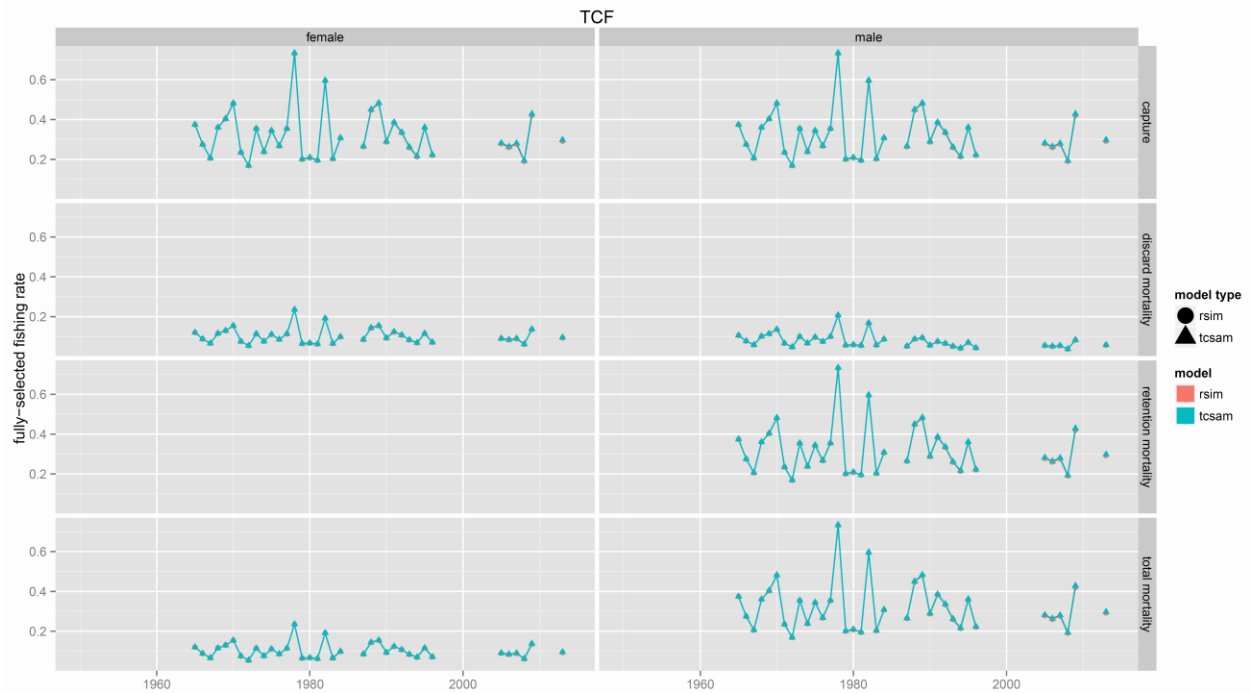Fig. 6d.28. Comparison of estimated ("tcsam") and true ("rsim") size-averaged annual survey Q's.

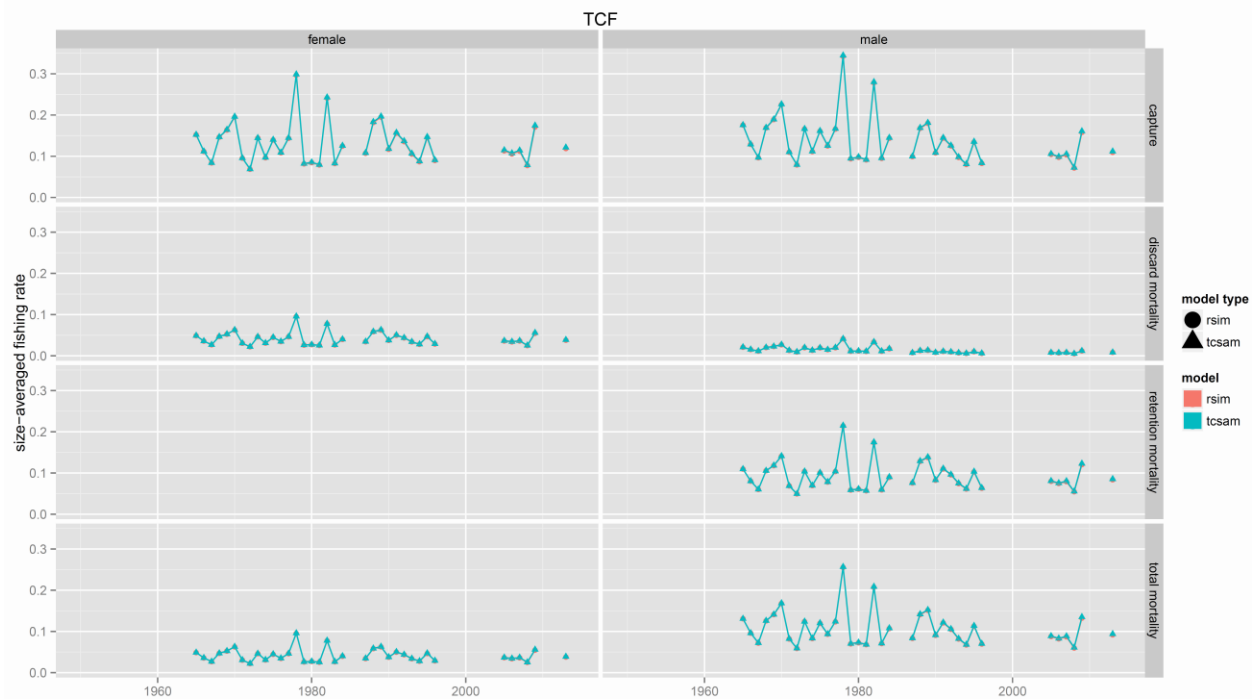Fig. 6d.29. Comparison of estimated ("tcsam") and true ("rsim") fully-selected annual TCF fishing rates.

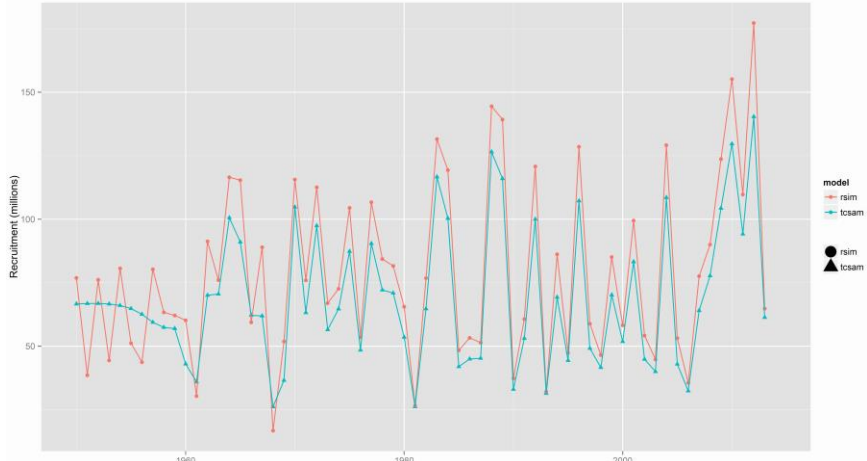Fig. 6d.30. Comparison of estimated ("tcsam") and true ("rsim") size-averaged annual TCF fishing rates.

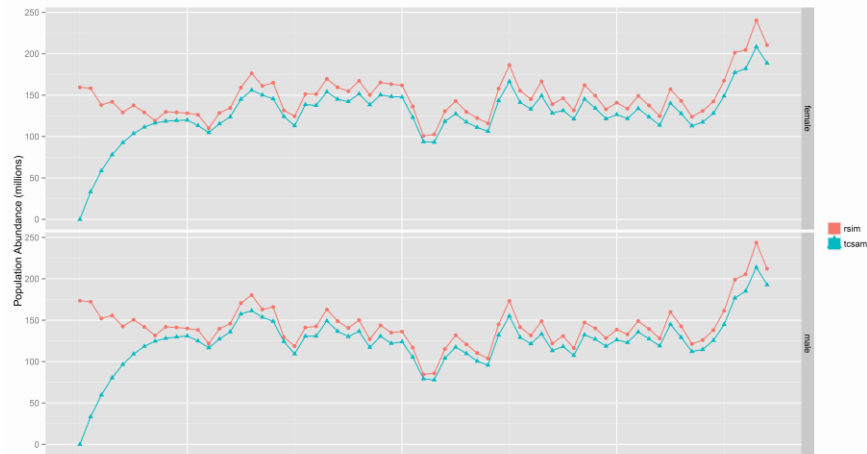Fig. 6d.31. Comparison of estimated ("tcsam") and true ("rsim") recruitment.

Fig. 6d.32. Comparison of estimated ("tcsam") and true ("rsim") population abundance.
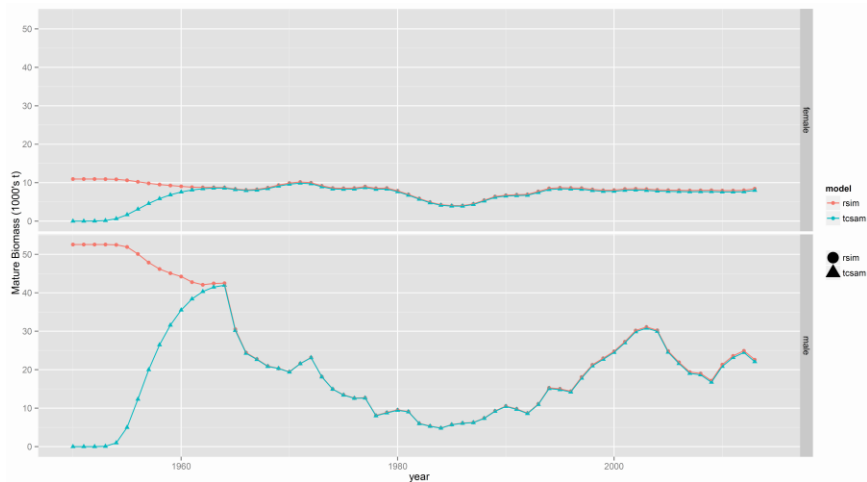

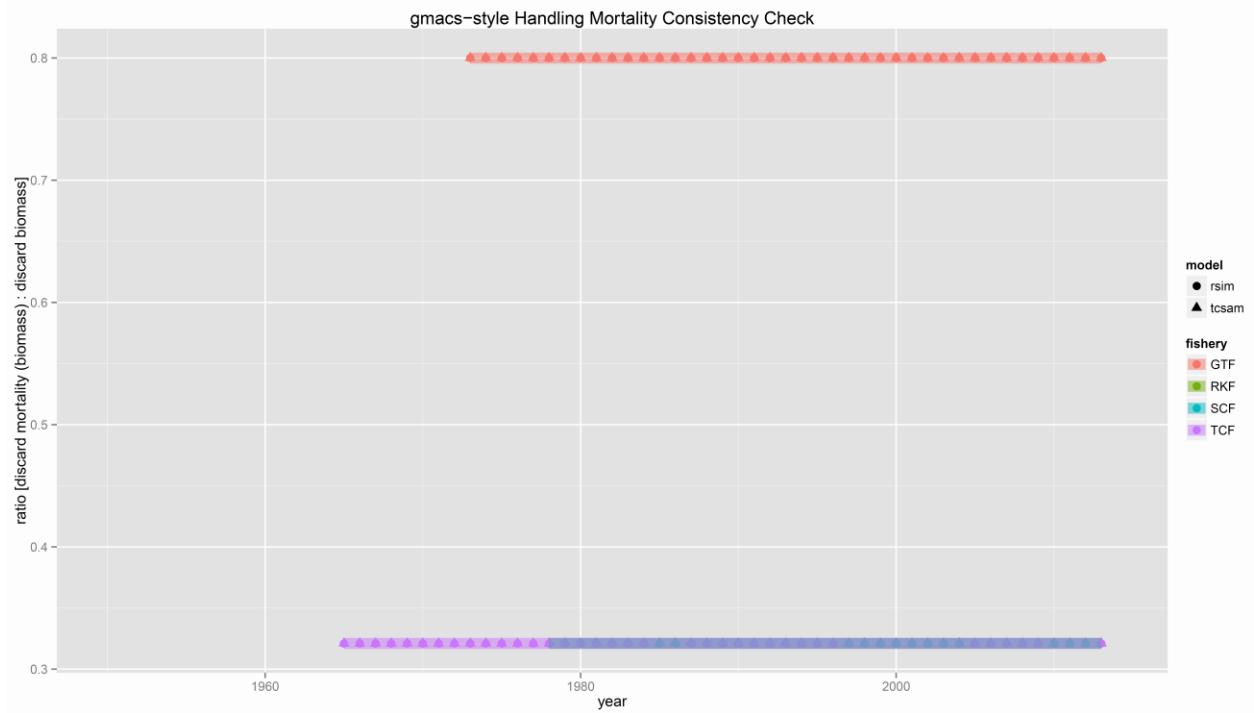Fig. 6d.33. Comparison of estimated ("tcsam") and true ("rsim") mature biomass.

Fig. 6d.34. Check on discard mortality for consistency of Gmacs fishery equations.